The Effects of Dynamic Loading on Rut Development

Development of a rut-depth model based on empirical data, introducing dynamic loading as prediction variable.

R.W. van Dijk

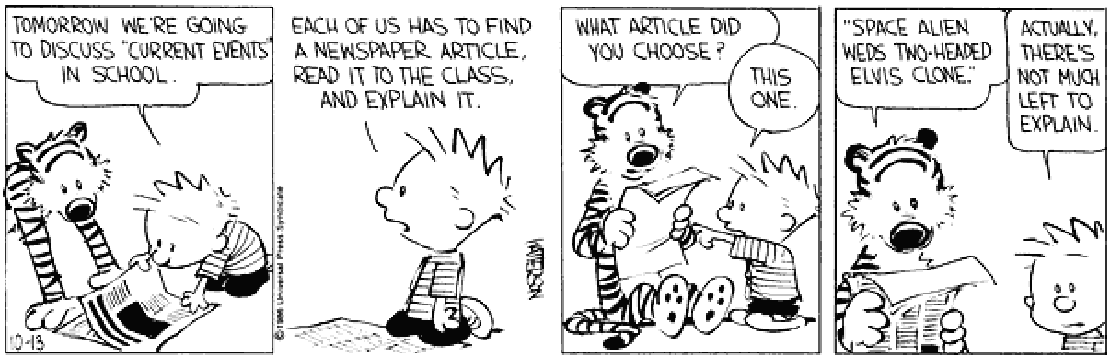

Bill Waterson (1986)

ACKNOWLEDGEMENTS

This report is the result of research done in the 1997 at the Delft University of Technology, Faculty of Civil Engineering. The research was done to obtain my degree as Civil Engineer at the above-mentioned institution.

I would like to thank Prof.dr.ir A.A.A. Molenaar for his time and valuable advice on this project. Further gratification goes out to all the staff of the laboratory as they made my stay very pleasant and educational. I would like to thank my fellow students of room 2.08 and 2.07 especially Peter "*knuckle man*" Bhairo and Tony "*Montana*" Visser for the many pleasant conversations and intriguing "*brainstorm sessions*".
To my girlfriend Irene: thanks for all your patience hope to see you soon again. I would also like to thank my parents for making this all possible.

Ricky van Dijk
Delft, 1 November 1997.

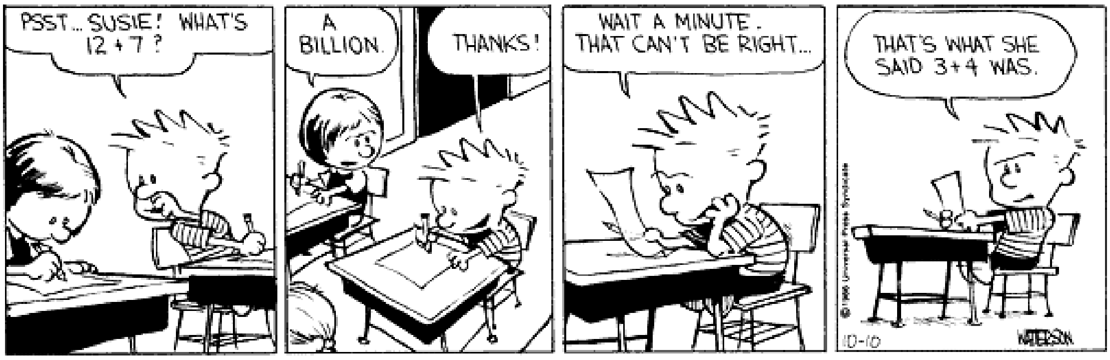

Bill Waterson

SUMMARY

Rutting is the phenomenon where "g*utters*" appear in the asphalt pavement as the result of densification, viscous- and plastic deformation introduced by traffic loads. The driver safety and comfort are the two aspects that are the most influenced by this form of damage. Rainwater gets collected in the rut and can result in "*aquaplaning*" in which a thin film layer of water is formed between the vehicle's tire and the road. At this point the driver has no control over his vehicle and is exposed to great danger. The Dutch road authorities have come up with guidelines for maximum rut-depth in order to lower the risk of "*aquaplaning*" to the road users. Following their own guidelines the road authorities are compelled to perform maintenance on those roads that exceed the rut-depth guidelines. These road maintenance tasks are becoming more difficult as the traffic intensifies and as the public is getting weary of all the delays that result from these road maintenance activities.

Road engineering has long dealt with the problem of predicting rut development. A number of mechanistic and empirical models were developed in the course of time that are able to make fairly reliable estimates of the rut development. The key word is estimate. A number of assumptions had to be made in the models concerning traffic loading, the material characteristics and stress conditions in the pavement structure. These assumptions resulted in the introduction of uncertainties in the model that in their turn effect the accurateness of the prediction. One of the assumptions concerns the loading of the pavement. All of the existing models assume that the traffic loading is constant and equal to the static weight of the vehicle. This assumption is only valid if the pavement surface is perfectly smooth. In-service pavements will always have some amount of longitudinal unevenness. A vehicle that travels over such a road will react to the road's unevenness by rapidly moving up and down, introducing vertical acceleration that effect the forces that occur between the tires and the road.

The goal of this research program was to research the effect that dynamic vehicle loading on rut development. The relationship will be researched using data obtained from test-sections that are frequently inspected in the SHRP-NL project. Regression analysis was used as the method for finding the relation between rut development and dynamic vehicle loading.

The first step in the study was to calculate the dynamic vehicle loads using a software program that is developed by the author with the sole purpose of simulating vehicle

responses and the resulting tire forces. The simulation was done for forty secondary roads in the Netherlands. The standard deviation of the dynamic vehicle loads were calculated and added to the regression analysis as a rut-explanation factor. Other variables that were used in the regression analysis were the maximum deflection as measured by a Falling Weight Deflectometer, the age of the overlay, the number of equivalent axle load passages and the type of base material.
The regression analysis showed that, based on the sample of test sections that were used in this study, that the effect of dynamic vehicle loading couldn't be proven. The regression did show that rut development is strongly influenced by the type of base material that is used in the pavement structure and the age of the overlay. The strong dependency of rut development on the age of the material is caused by the process called aging, in which the stiffness of the asphalt increases in the course of time. The increase in stiffness results in a material that is more resistant to rutting.

Table of contents

Bill Waterson (1986)

CHAPTER 1 INTRODUCTION

Rut-depth is defined as the transverse unevenness in the road profile. Rutting is considered a major defect and can have a significant effect on driving safety (*when the ruts are filled with rainwater it could result in aquaplaning*) and driving comfort. It becomes obvious that an accurate prediction of rut-depth development is very important to both the user and road authorities.
In this chapter a short description of the principle of available rutting is described as well as the parameters that influence the rutting behavior. It will be shown that normally the effect of dynamic loading is ignored and it will be explained why dynamic loading effects should be taken into account in the prediction of rutting.

1.1 Current Rut Development Models

Rutting is the result of densifications, viscous and plastic deformation of the materials that are used in the pavement structure due to traffic loading. Viscous plastics flow of the material primarily causes rutting in the asphalt layer. It is therefore necessary for any rut development model to include the loading conditions and the characteristics that are used in the pavement structure.
A number of rut prediction models have been developed in the course of history that, although they appear different, can be described by means of the following general model (*see equation (0-1)*).

$$U_p = a \cdot N^b \qquad (0\text{-}1)$$

where: U_p = permanent deformation,
a, b = constants that are depended on the loading conditions and describe material characteristics of pavement structure,
N = number of vehicle loads.

Two approaches are used to determine the values for the a and b parameters namely:
- The parameters are calculated using extensive mathematics and material testing,
- The parameters are estimated using regression analysis.

Finding the right values to describe the material characteristics and stress conditions in the pavement can proof to be a very difficult task. The complexity of the task of predicting the exact values of the different parameters in the rut development model has forced the researchers to introduce some simplifications into the model. These simplifications have led to the introduction of uncertainties in the rut development model, which lead to errors in the predictions.

1.2 Research Goals

A number of assumptions are made in the analysis of stresses and strains in the pavement. These assumptions have their effect on the rut development model, as explained in paragraph 1.1. One of these assumptions is that the loading of the pavement by a vehicle is constant regardless of the speed or conditions of the pavement and equals its static load. This assumption is only valid if the pavement surface is perfectly smooth. In-service pavements will always show some longitudinal unevenness. Normal vehicles will undergo vertical vibrations if subdued to these variations in the pavement surface. This vertical vibration will in its turn lead to a variation of the contact forces between tires and road. This dynamic vehicle loads could result in an increase in damage of the pavement (*see 0*).

"*The goal of this study is to determine the effect of introducing a variation in loading, (dynamic vehicle loading) on rutting*"

1.3 Research Method

The effect of the dynamic vehicle loading will be studied using regression analysis. This method requires the input of many data points that consist of variables that can explain rutting as well as actual rut-depth measurements. These data are obtained from measurements that are done on actual in-service pavement in the Netherlands as part of the SHRP-NL program. The actual regression analyses are done using the shareware version of the computer program DataFit©, which makes it possible to do multiple-nonlinear regression analysis.

1.4 What is in this Report

This report is divided in three parts. The first part (*chapter 2*) is a literature review of previous research. The second part (*chapter 3 and 4*) deals with vehicle simulation on SHRP-NL test-sections, which are used in this study and a description of these test-sections. The third part (*chapter 5 and 6*) of this report is dedicated to the development of a rut-depth prediction model, that is based on data described or gathered in the second part of this report.

CHAPTER 2 PREVIOUS RESEARCH

This chapter will discuss two types of approaches that have been used to evaluate the effect of dynamic vehicle loads on pavement wear. The first method that is described in this chapter is the road stress factor developed by Eisenmann. This method can best be described as a "*quasi-static*" approach to dynamic vehicle loading in which the vehicle loading is assumed to be constant along the road profile but dependent on the longitudinal unevenness of the road. The other methods that are described in this chapter are the "*full-dynamic*" approaches by Collop and Huurman, in which the damage due to the passages of a single vehicle is calculated at discrete points along the road profile.

2.1 The road stress factor

The road stress factor describes the increase in vehicle loading as a function of the longitudinal unevenness of the road profile. Eisenmann [3][4] assumed that the dynamic loads are distributed evenly along the pavement and that the damage has a fourth power relationship with the vehicle load. The power of 4 is based on the "*fourth-power-law*" that is a result form the AASHO full-scale test of the late 50's that stated that pavement damage is inversely proportional to the axle weight raised to the forth power. Equation (2-1) shows the definition of the road stress factor as developed by Eisenmann.

$$\Phi = E\left[P(t)^4\right] = (1 + 6 \cdot s^2 + 3 \cdot s^4) P_{stat}^4 \qquad \textit{(0-1)}$$

where: E = expectation factor,
s = the coefficient of variation of the dynamic load $P(t)$ often known as the "*Dynamic Load Coefficient*",
P_{stat} = mean value of vehicle load P

The factor $\nu = (1 + 6 \cdot s^2 + 3 \cdot s^4)$ is known as the "*Dynamic Load Stress Factor*" and defines the additional damage due to dynamic loads. Eisenmann later modified equation (2-1) to account for different wheel configurations and tire contact pressures (*see equation 2-2*).

$$\Phi' = \nu \cdot \left(\eta_I \cdot \eta_{II} \cdot P_{stat}\right)^4 \qquad \textit{(0-2)}$$

where: ν = dynamic load stress factor,
η_I = constant which account for wheel configuration (single or dual),
η_{II} = constant which account for tire contact pressure.

Note that η_I and η_{II} can be considered "penalty" or "bonus" factors, depending on the suspension type or axle configuration. For example, an OECD report recommended η_I = 1.0 for twin and 1.3 (*penalty*) for single tires, while Eisenmann recommended η_I = 1.0 for single tires and 0.9 (*bonus*) for dual tires.

For typical highway conditions of unevenness, Sweatman [10] measured values of ν in the range of 1.11 to 1.46, depending on the suspension type.

The road stress factor states that the vehicle loading of the pavement is constant along the pavement and depended on the unevenness of the pavement profile. The increased of the vehicle loads were used as input to fatigue damage relationships. Damage calculations that where done using the Road Stress Factor estimated an overall increase in fatigue damage in a range of 20% to 40%.
Although the Road Stress Factor in a very simple way of incorporating dynamic tire loads into design methods, it does have a few shortcomings. One of the main disadvantages of the road stress factor approach is the use of the “fourth power law”, which has been subjected to considerable criticism.

2.1.1 Conclusion on the Quasi-Dynamic approach

The quasi-dynamic approach shows a significant increase in pavement damage due to the application of dynamic loads instead of static loads. The quasi-dynamic approach predicts an evenly distributed (*average*) damage accumulation along the pavement. This is due to the fact that in the quasi-dynamic approach the increased dynamic loads are considered not to vary along the wheel path. The advantage of such an assumption is the ease with which this approach could be implemented into existing design procedures.

2.2 The Full Dynamic Approach for Asphalt

The following paragraphs will discuss two methods that use the "*full-dynamic*" approach to determine the effect of dynamic vehicle loading on the damage accumulation of pavement structures. The first model to be described was developed by Collop. This model was developed to simulate the wear of an asphalt-paved road. The second model was developed by Huurman and simulates the damage development of a concrete element pavement.

2.2.1 The Asphalt Pavement Model

The first of the "*full-dynamic*" models is the one that is developed by Collop and Cebon in the United Kingdom [2]. This model is quite detailed as it incorporates a great number of variables that are known to influence the performance of an asphalt paved road. Figure 2-1 shows a diagram of the model and all the different modules that make up the simulation. The different parts of the model will be discussed in the following paragraphs.

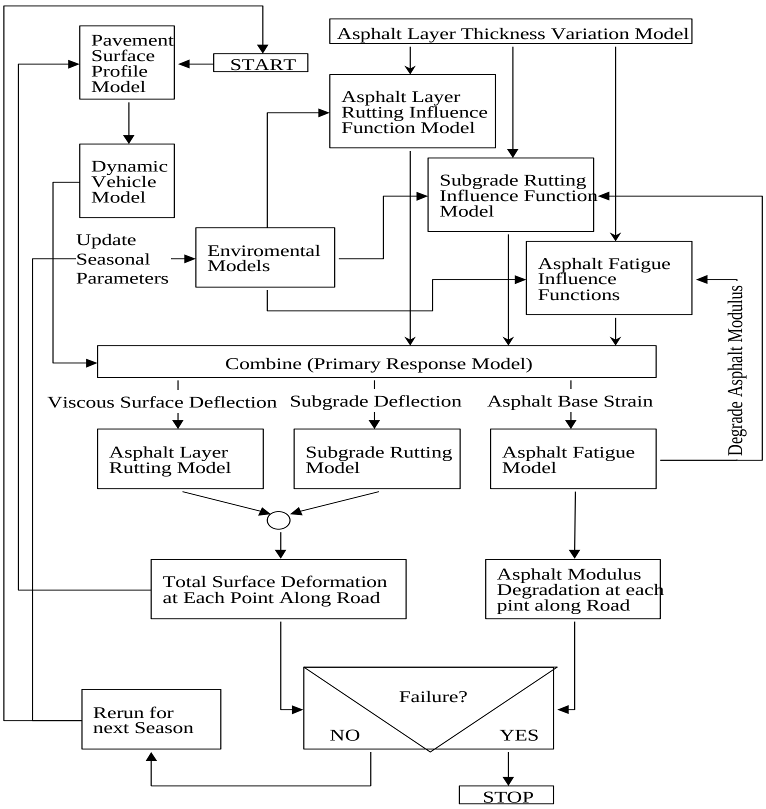

Figure 0-1 Asphalt Pavement Model

Vehicle simulation

The first module of the model concerns the simulation of a vehicle on a given road. Two elements are needed to complete the simulation namely a vehicle model and a road profile. For the purpose of simulating a vehicle, a "*quarter car*" (*see Figure 2-2)* mathematical model was developed.

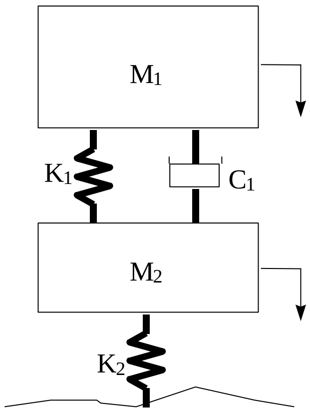

Typical Parameters	Steel	Air
m_1	4500 [kg]	4500 [kg]
m_2	500 [kg]	500 [kg]
k_1	1.00 [MN/m]	0.40 [MN/m]
c_1	20 [kNs/m]	20 [kNs/m]
k_2	2.00 [MN/m]	2.00 [MN/m]

Figure 0-2 Quarter-Car Vehicle Models used in Asphalt pavement model

The mathematical vehicle model makes it possible to calculate the vehicle reaction to vertical excitement of the tires as a result of the longitudinal unevenness of the pavement. The combination of the vehicle model and the road profile produces the vertical tire forces at discrete points along the wheel track.

Primary response model

A modified version of the VESYS IIIA quasi-static pavement model was used to calculate the required primary pavement responses. VESYS IIIA models the pavement as a multi-layered visco-elastic system supported by a semi-infinite subgrade. Contact between the tire and pavement is modeled as a circular contact area. All pavements that were investigated in this model consisted of an asphalt layer, a granular subbase and a subgrade layer. The primary-response model requires the elastic properties and the thickness of each layer as input.

Elastic properties

The elastic properties were first corrected by correcting the *PI* of the asphalt for "*short term aging*" using the following equations developed by Brown and Burton [1].

$$P^{(R)} = 0.65 \cdot P^{(I)} \tag{0-3}$$

where $P^{(I)}$ = initial bitumen penetration [mm],
$P^{(R)}$ = recovered bitumen penetration [mm].

$$T_{RB}^{(R)} = 98.4 - 26.35 \cdot \log(P^{(R)}) \tag{0-4}$$

where: $T^{(R)}_{RB}$ = recovered softening temperature Ring and Ball [^{0}C].

$$PI^{(R)} = \frac{27 \cdot \log(P^{(I)}) - 21.65}{76.35 \cdot \log(P^{(I)}) - 232.82} \quad (0\text{-}5)$$

where: $PI^{(R)}$ = recovered Penetration Index [-].

"*Long term aging*" was added to the model by using the relation developed by Verhasselt and Choquet [10] (*see equation* (2-6)).

$$T_{RB}^{(R)}\Big|_{t1} = T_{RB}^{(R)}\Big|_{t1} + \sqrt{\Lambda t} \quad (0\text{-}6)$$

where: $T_{RB}^{(R)}|_{t1}$ = Softening Ball and Ring Temperature resulting form aging [^{0}C],
Λ = reaction constant [C^2/hr], depending on the type of bitumen.
$1.2 \cdot 10^{-3} < \Lambda < 2.1 \cdot 10^{-3}$.

Several studies have shown that in-service pavements have a significant relationship between the deflection and the long-term pavement behavior indicating a decrease in stiffness of the asphalt material in time. Collop developed a relationship that could predict the degradation of the asphalt as a function of time [2]. Figure 2-3 shows the development of the stiffness as a result of short- and long-term aging and degradation of the asphalt modulus.
This stiffness development in time was thus used in combination with the VESYS IIIA computer program to calculate the responses of the pavement at any moment in time.

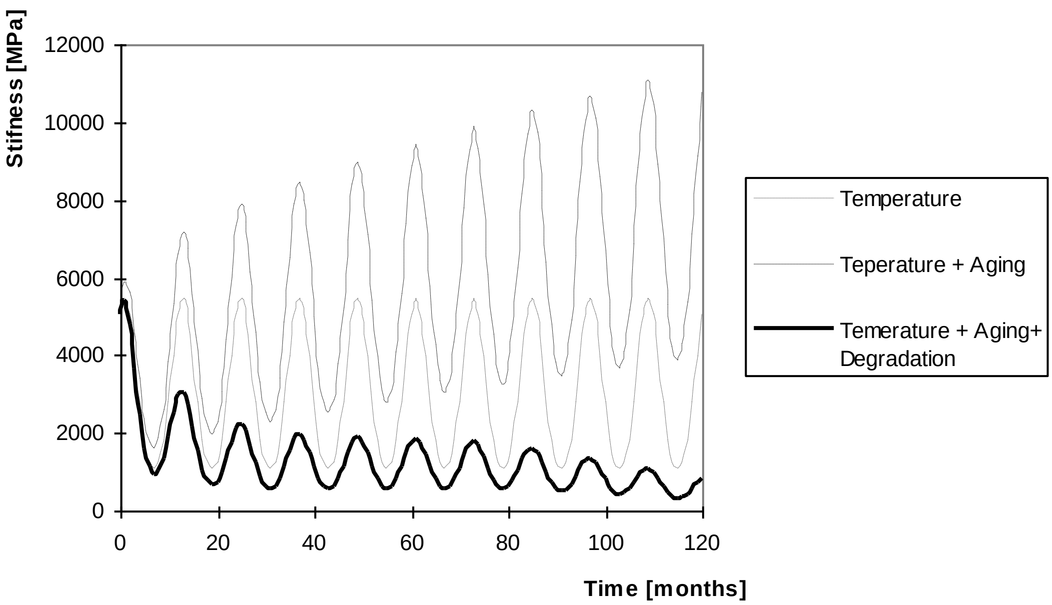

Figure 0-3 asphalt stiffens in relation to its age.

Rut Development

Permanent deformation of the pavement due to a certain load is calculated using VESYS IIIA.

Rutting is calculated using equation (2-7). A point on the road undergoes an increase in strains as a vehicle approaches, building up to a maximum strain level as the vehicle is directly above this point and then decreases as the vehicle travels away. In the model by Collop [2] the total rut depth increase is a result of all the strain levels that a certain point on the road undergoes

$$z_\infty = \frac{F}{v} \int_{-x_0}^{x_0} h_\infty(x) \cdot dx \qquad (0\text{-}7)$$

where: z_∞ = the total deformation as a result of one vehicle passage [mm],
F = applied load [kN],
v = vehicle speed [m/s],
x_0, $-x_0$ = distance over which point x is influenced by vehicle load [m],
h_∞ = the permanent vertical displacement at distance x of from the point of
load application [mm].

Permanent deformation that is calculated using equation (2-7) is proportional to the static load F, and inversely proportional to vehicle speed v.

Subgrade Rutting

The permanent deformation model used in the simulation also incorporated a subgrade rutting based on vertical strains in the subbase.

$$\delta_i = L_1 \cdot \varepsilon_i^{L_2} \qquad (0\text{-}8)$$

where: δ_i = incremental permanent deformation in unbound layers [mm],
ε_I = vertical subgrade compressive strain [‰],
L_1, L_2 = material parameters [-]

The vertical strain in the subgrade is calculated by means of the VESYS IIIA multi-layered vico-elastic program.

The total permanent deformation of the pavement surface caused by a single vehicle passage is the sum of the deformations calculated by equations (2-7) and (2-8).

Fatigue damage

The "*Wöhler approach*" (*an empirical approach see equation (2-9)*) was used in Collop's model to relate strains at the bottom of the bound construction to fatigue life.

$$N_f = k_1 \left(\frac{1}{\varepsilon} \right)^{k_2} \qquad (0\text{-}9)$$

Where: N_f = number of strain applications to failure [-]
ε = strain at the bottom of the bound layer [mm/mm]

k_1, k_2 = factors depending on the composition and the properties of the asphalt mix [-].

The parameter k_1 and k_2 are usually determined using fatigue tests. A common test is the 4-point bending test. Empirical relationships for k_1 and k_2 were developed for typical British asphalt mixes (*see equations (2-10) and (2-11)*).

$$\log(k_1) = 14.39 \cdot \log(V_B) + 24.2 \cdot \log(T_{RB}^{(I)}) - 46.06 \qquad (0\text{-}10)$$

$$k_2 = 5.13 \cdot \log(V_B) + 8.63 \cdot \log(T_{RB}^{(I)}) - 15.8 \qquad (0\text{-}11)$$

where: $T^{(I)}_{RB}$ = initial ring and ball softening temperature of the bitumen [^{0}C],
V_B = percentage volume of bituminous binder [%].

Using VESYS IIIA as a method to calculate the strains in the pavement structure, it is now possible to calculate the expected number of vehicle passes until fatigue using equation (2-9). The fatigue damage at each point along the road due to the passage of a vehicle was estimated using "*Miner's law*", which assumes a linear accumulation of damage.

$$D = \sum_{i=1}^{j} \frac{n_i}{N_{f,i}} \qquad (0\text{-}12)$$

where: D = accumulated damage [-],
n_i = number of passes of vehicle type i [-],
N_f = number of vehicle passes to failure of vehicle type i [-].

A parametric test

Collop did some parameter studies in order to get a general feeling for the simulations. Four different case studies were used to determine the effect of variations of the asphalt construction and vehicle loading.

Case (1)	Initial profile (2)	Asphalt Thickness (3)	Vehicle Loads (4)
0	Smooth	Uniform	Static
1	Random	Uniform	Dynamic
2	Smooth	Random	Static
3	Random	Random	Dynamic

Figure 0-4 Different Operating Cases for parameter study

The results of the full simulations are given in Figure 2-5 to Figure 2-7. The line representing case_0 is the damage accumulation that would be predicted by the standard methods of pavement design (*not taking into account the dynamic loads and variations in the pavement structure*).

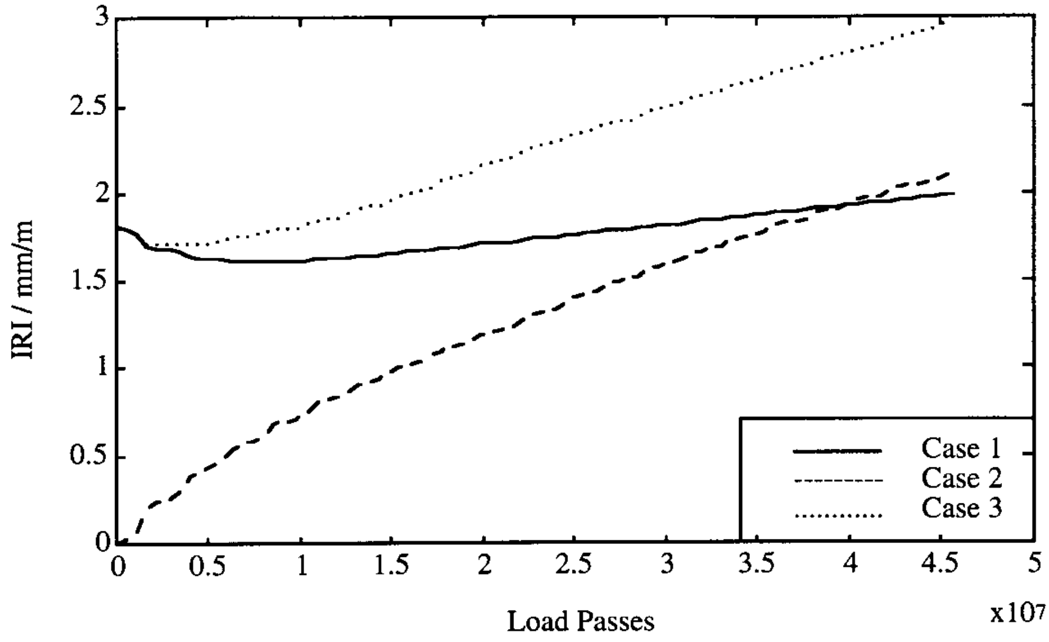

Figure 0-5 development of IRI as function of load passes

In this figure the development of the *IRI* value for case 0 is not plotted because it did not change during the course of time. Case 2 shows the greatest change in *IRI* value. This indicates that pavement deterioration is greatly dependent on the variations in asphalt layer thickness.

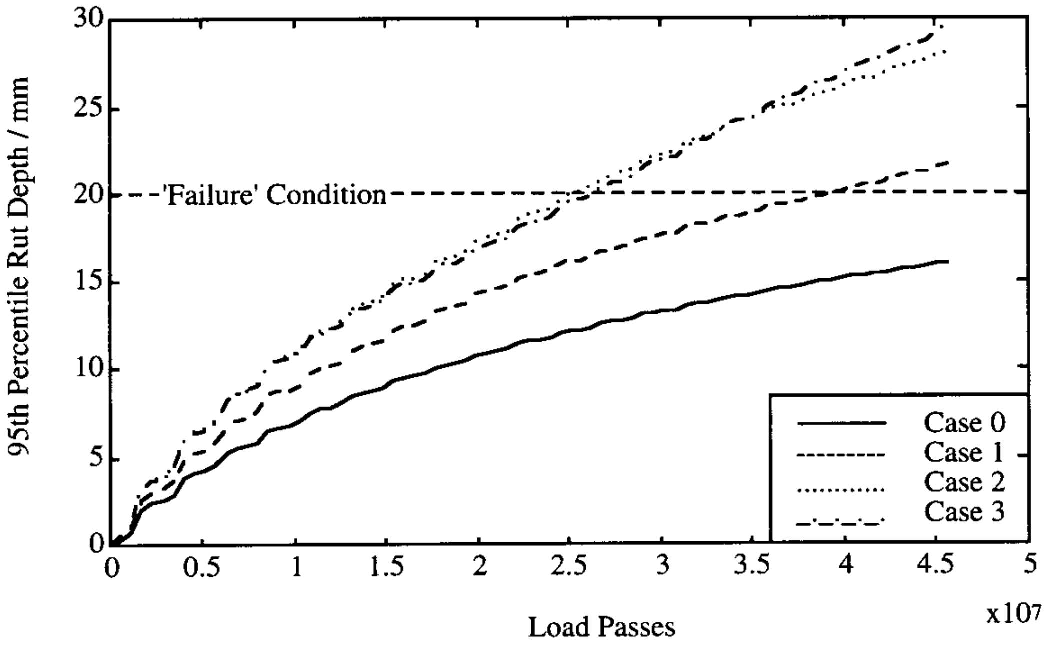

Figure 0-6 development of rut-depth as function of load passes

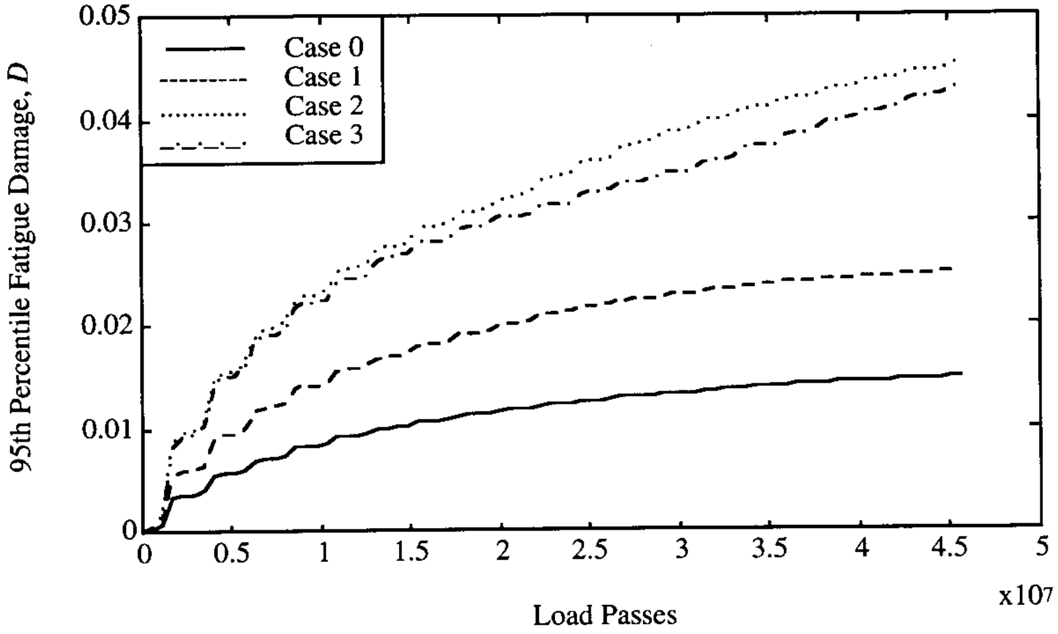

Figure 0-7 development of fatigue damage as function of load passes

Figures 2-6 and 2-7 show that the rut-depth increases as the variation in pavement structure and loading increases. This can be explained from the deformation models that were used in this simulation. The models stated that an increase in applied forces would lead to an increase in damage. The plots also show that the asphalt thickness of the pavement has a great influence on the damage development (*Case 2*).

2.2.2 Concrete Element Model

Huurman [5] developed a "*Full Dynamic*" model that simulates the damage accumulation of a concrete block pavement. This model is very similar to the model of Collop with the exception that the rut development is the result of deformation in the unbound base only and that the pavement material (*concrete*) is not effected by fatigue damage. Another difference between both the models is that Huurman used a "*half car*" mathematical vehicle model instead of a "*quarter car*" model.
The following paragraph will discuss the simulation model, the mathematical vehicle model and the primary response model that make up the Huurman model.

The Simulation Model
Figure 0-8 shows the flow-chart of the simulation method, which was used in the concrete element model. The method to calculate the development of the longitudinal profile consisted of a "*half car*" vehicle model and a rut-depth prediction model. The "*half car*" vehicle model was used, in combination with the longitudinal profile, to provide the tire forces needed as input to the rut-depth model.

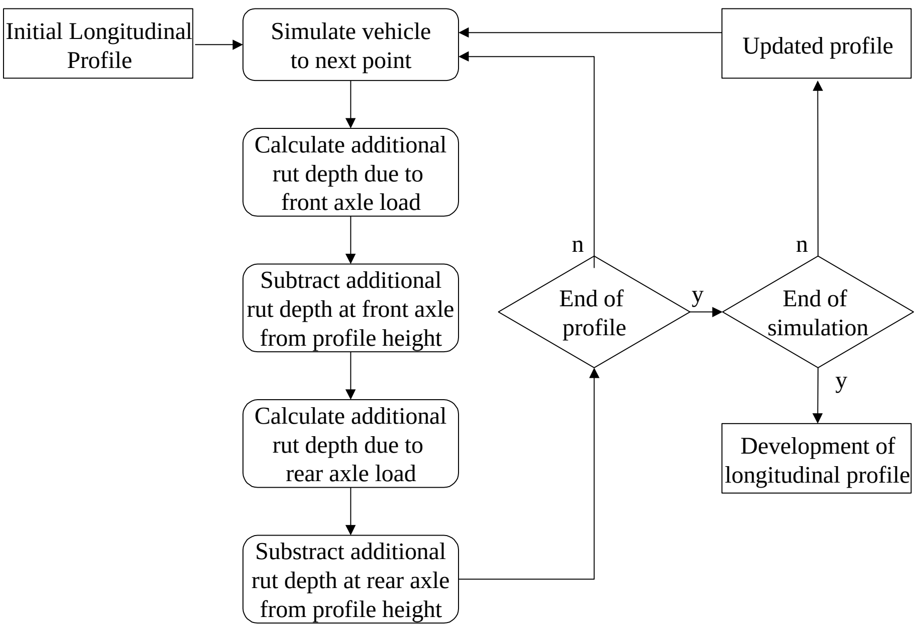

Figure 0-8 Concrete Elements Model

The chart shows that the road profile is updated twice on every passage of a vehicle. This is the result of using the "*half car*" vehicle model. As the first axle of the vehicle travels over the pavement it will induce some damage that will effect the response of the rear axle of the vehicle. The simulation is run until the pavement reaches the end of it functional life.

Vehicle Simulation

The use of a "*half car*" vehicle model (*see Figure 0-9*) was done to account for extra dynamic wheel loads as a consequence of vehicle carriage mass inertia. Vehicle simulations done with the "*half car*" model showed that the dynamic loads of the front and rear axle do show a difference in the loads that are applied to the pavement.

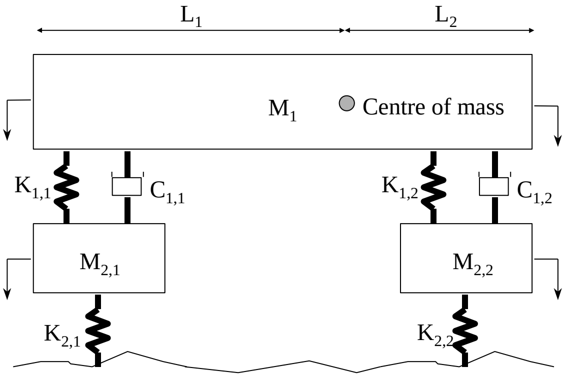

M_1 = 5.500 [kg]
J_1 = 9.640 [$kg \cdot m^2$]
M_2 = 800 [kg]
M_3 = 1.300 [kg]
$K_{1,1}$ = 430.00 [N/m]
$K_{1,2}$ = 700.000 [N/m]
$C_{1,1}$ = 30.000 [$N \cdot s/m$]
$C_{1,2}$ = 30.000 [$N \cdot s/m$]
$K_{2,1}$ = 1.500.000 [N/m]
$K_{2,2}$ = 4.000.000 [N/m]
L_1 = 1.02 [m]
L_2 = 2.18 [m]

Figure 0-9 Half-Car vehicle Model

Figure 0-10 shows the result from a *"half-car"* simulation over a speed bump. As can be seen, the plots of the dynamic tire forces along the wheel-path differ from each other. This simulation was done using a two-axle truck with a front axle load of 69.9 [kN] and a rear axle load of 100 [kN]. As the front wheel reaches the speed bump in the road, it is pushed upward, this causes the vehicle mass to rotate, pushing down on the rear axle hence increasing the rear axle load even before it reaches the bump on the road.

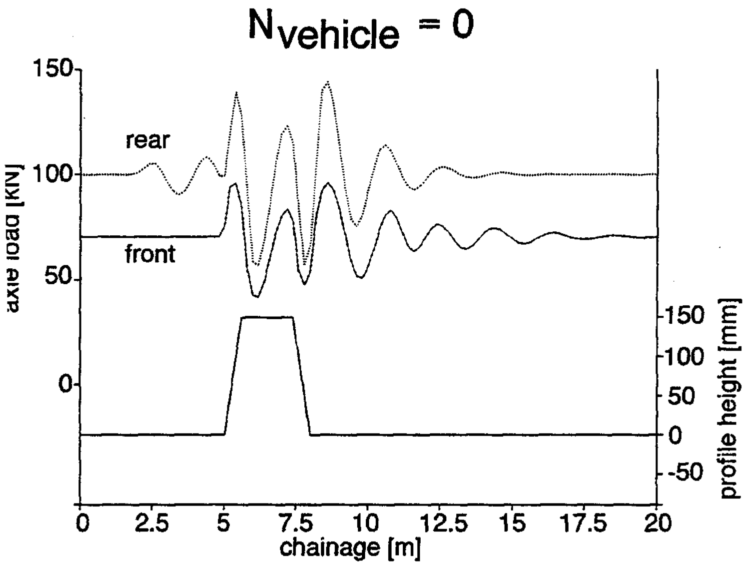

Figure 0-10 Dynamic loads of half car simulation over road bump

Primary Response Model
The rut development model that was developed by Huurman is represented in equation (2-13 to 2-15).

$$RD_a[N_{st}] = RP \cdot \left(a_p \cdot \left(\frac{N_{st}}{1000} \right)^{b_p} + c_p \left(e^{\frac{N_{st}}{1000} \cdot d_p} - 1 \right) \right) \tag{0-13}$$

$$N_{eq} = \frac{1}{100} \sum_{i=1}^{vnu} \left(\%_i \left(\frac{Lf_i}{AL_{st}} \right)^{m_l} \times \left(\frac{\sigma \cdot f_{c,i}}{\sigma_{c,st}} \right)^{m_c} + \%_i \left(\frac{Lr_i}{AL_{st}} \right)^{m_l} \times \left(\frac{\sigma \cdot r_{c,i}}{\sigma_{c,st}} \right)^{m_c} \right) \tag{0-14}$$

$$N_{st} = N \times N_{eq} \tag{0-15}$$

where: $Rd_a[N_{st}]$ = absolute rut depth after N_{st} standard axle load [mm],
a_p, c_p = pavement properties [mm],
b_p, d_p, m_i, m_c, RP = pavement properties [-],
Al_{st} = standard axle loads which equals $2 \cdot L_{st}$ [kN],
Lf_1, Lr_i = static front respectively rear axle load of vehicle *i* [kN],
N_{st} = number of equivalent axle loads [-],
$\%_i$ = percentage of vehicle i in traffic [-],
vnu = number of different vehicles in traffic [-],
N_{eq} = number of equivalent standard axle loads [-],
N = number of vehicle passes [-].

The Huurman model makes it possible to predict the absolute rut depth as a function of the number of vehicle passages.

Simplification of the simulation
The problem with the full simulation method, is the large amount of time needed to simulate the whole design live of the pavement structure. Simulation would run for several days. Huurman tried to decrease the simulation time by simplification of pavement and vehicle models. Linearizing both models did simplify the simulation and decreased the time needed for a full simulation.

Linear vehicle response model
Vehicles tend to show a linear response to longitudinal unevenness. This linear response can be directly derived from the way the vehicle model is build, namely, using only linear-elastic or linear-viscous elements to model the springs and shock absorbers. In Huurman's approach, it was assumed that the amplitude of the tire forces is linear dependent on the amplitude of unevenness. The road profile was analyzed using the Fourier method, braking up the profile into wavelengths and their corresponding amplitudes. Calculating the dynamic forces then becomes a simple multiplication of the amplitude of a certain wavelength and the reaction of the vehicle to that wavelength (*see equation (2-16) and 2-17)*).

$$Aff_{\lambda,i}[N_{st}] = Au_{\lambda}[N_{st}] \times ff_{\lambda,i} \tag{0-16}$$

$$Afr_{\lambda,i}[N_{st}] = Au_{\lambda}[N_{st}] \times fr_{\lambda,i} \tag{0-17}$$

where: $Au_{\lambda}[N_{st}]$ = amplitude of wavelength λ after [N_{st}] standard axle loads [mm],

$Aff_{\lambda,I}[N_{st}]$ $Afr_{\lambda,I}[N_{st}]$ = Amplitude of dynamic component of the front or rear axle of vehicle type "i" as reaction to an unevenness with wave-length "λ" [kN],

$ff_{\lambda,i}$, $fr_{\lambda,I}$ = parameters which relates the amplitude of the dynamic component to the amplitude of unevenness [-].

The parameters $ff_{\lambda,i}$, $fr_{\lambda,i}$ are found by simulating a whole range of vehicle/speed combination on pure sines. Figure 2.11 is a graphic display of the way the simplification works. Vehicle response is calculated from the initial road profile using equations (2-16) and (2-17). The resulting axle loads are then transformed to a new profile by adding the initial profile with the incremental increase in rut-depth.

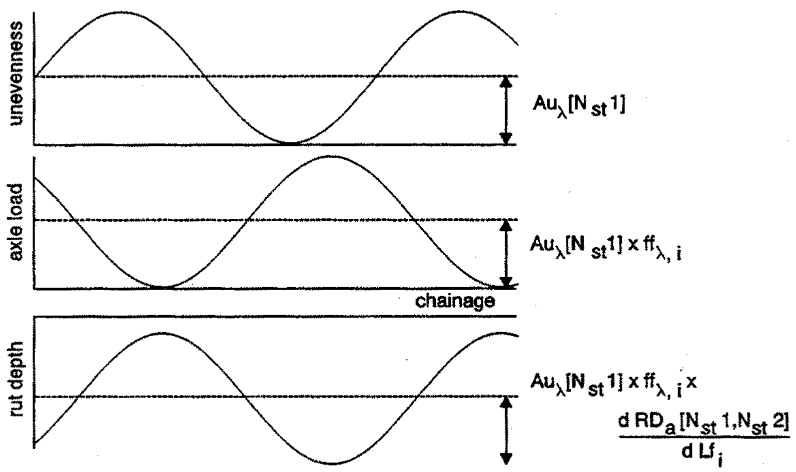

Figure 0-11 simplified interaction of road profile, vehicle response and rut-depth

A Parametric study

Three types of vehicles were simulated over a concrete block pavement. The first vehicle is the " standard 100 kN" vehicle. The second vehicle is called the "Standard Vehicle 100 [kN] 2xk" that has an increase in the tire stiffness to simulate over inflates tires. The shock absorber stiffness of the third vehicle, "Standard vehicle 100 [kN] c/3" is lowered to simulate a truck with worn shock absorbers.

	Standard Vehicle 100 [kN]	Standard Vehicle 100 [kN] 2 x k	Standard Vehicle 100 [kN] c / 3
front axle load [kN]	69.9	69.9	69.9
rear axle load [kN]	100.0	100.0	100.0
front axle spring stiffness [N/m]	430.000	430.000	430.000
rear axle spring stiffness [N/m]	700.000	700.000	700.000
front axle damper stiffness [Ns/m]	30.000	30.000	10.000
rear axle damper stiffness [Ns/m]	30.000	30.000	10.000
Front tire stiffness [N/m]	1.500.000	3.000.000	1.500.000
Rear tire stiffness [N/m]	4.000.000	8.000.000	4.000.000

Table 0-1 Vehicle characteristics

The three different vehicle were simulated on a given road profile to calculate the effect of dynamic tire forces on rut development and consequently the road profile. Introducing dynamic loads instead of static loads showed an increase in average rut-depth. Figure 2-12 shows the results of rut development using a full simulation of all three vehicles.

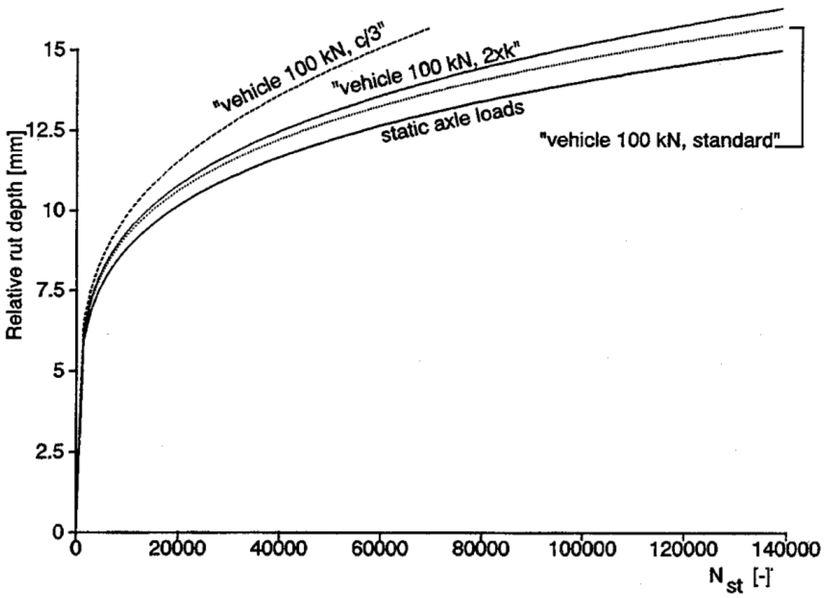

Figure 0-12 Rut developments as function of applied loads

2.2.3 Conclusions on Full Dynamic Approach

Both methods of full-dynamic approach seem to predict the same behavior in the accumulation of damage on a given road. They both predict the flattening of the short wave amplitudes, enlargement of long wave amplitudes.

Note that the full-dynamic methods are building upon damage relation commonly used in road engineering nowadays. The validity of the simulation models is therefore

strongly dependent on the validity of these relationships. A strong point of the models is that both models make it easy to incorporate new insights into pavement behavior. Both models predict an increase in pavement damage, which can exceed the design value, at discrete points along the pavement. The use of the full-dynamic approach requires a whole new method of describing and evaluating road damage, as road damage is now localized. New design criteria would have to be in such a form as " Design a road, which has a XX% chance that XX% of road surface is not damaged beyond a XX value".
Although both models give a very detailed overview of the damage development on road pavements, the application of the models is still very limited. Both models require very detailed information concerning road pavement characteristics, which are not always available.

Bill Waterson

CHAPTER 3 DYNAMIC VEHICLE LOADING

Dynamic tire forces are generated when a vehicle travels over an uneven pavement surface. The reaction of the vehicle is dependent on the properties of the vehicle itself (*e.g. mass*, *speed*) and the irregularities that occur on the road.
This chapter will deal with the estimation of these forces by means of simulation.

3.1 Mathematical Vehicle Model

Everyday traffic shows a wide variety of vehicle shapes and types that result from the different demands that are made on the vehicle. Personal cars are used for the transportation of people, and trucks are used to transport freight. Although vehicles tend to show a great variety in the way they appear, they still show a similarity in the way the different parts of the vehicle operate and interact. All vehicles are made up of the following building blocks:

- motor (electrical, combustion, etc.) to provide the necessary energy to move the vehicle,
- chassis, which carries the vehicle weight and serves as a platform on which other parts of the vehicle (carriage, transmission, etc.) are mounted,
- suspension, which main task is to provide some comfort to the passengers, and improves the road-handling qualities of the vehicle,
- tires, (usually inflatable) which provide the necessary contact between the vehicle and the road.

A quarter car vehicle model is chosen in this study to represent the actual vehicle. As only the vertical tire forces are of interest in this study, the model is simplified to incorporate only those element of a vehicle that greatly effect the tire forces. (*See Figure 0-1*). Another restraint in the detailing is the fact that the road profiles that are used in this simulation are two-dimensional. This excluded all three-dimensional vehicle models for use in the simulation.

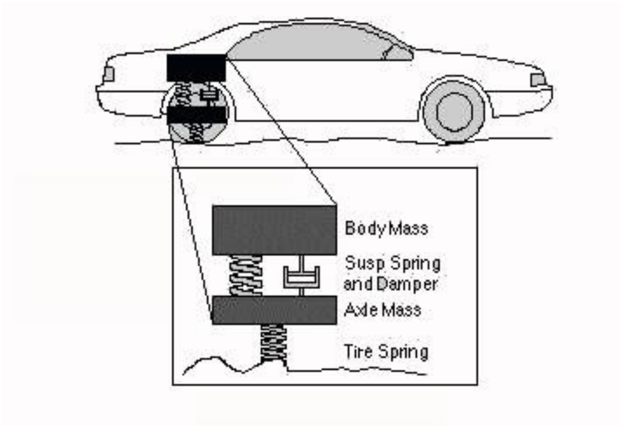

Figure 0-1 Quater Car Model

Figure 0-1 represents the model that is to be used in this study. The figure clearly shows how the different parts of the vehicle are schematized to two masses that are connected to each other by springs and shock absorbers. The tires on the car are also represented by a spring to model their elastic behavior.
By means of this model tire forces can be calculated using simple equations that need input parameters for the following vehicle characteristics: vehicles mass, axle mass, spring- and tire stiffness, speed and shock absorber stiffness. The equations that are necessary to determine the motions and resulting accelerations of the masses are taken from appendix B and shown below.

$$\begin{bmatrix} \frac{d^2 z_1}{dt^2} \\ \frac{d^2 z_2}{dt^2} \\ \frac{d^2 v_1}{dt^2} \\ \frac{d^2 v_2}{dt^2} \end{bmatrix} = \begin{bmatrix} 0 & 0 & 1 & 0 \\ 0 & 0 & 0 & 1 \\ -\frac{K_1}{M_1} & \frac{K_1}{M_1} & -\frac{C_1}{M_1} & \frac{C_1}{M_1} \\ \frac{K_1}{M_2} & -\frac{(K_1+K_2)}{M_2} & \frac{C_1}{M_2} & -\frac{C_1}{M_2} \end{bmatrix} \cdot \begin{bmatrix} \frac{dz_1}{dt} \\ \frac{dz_2}{dt} \\ \frac{dv_1}{dt} \\ \frac{dv_2}{dt} \end{bmatrix} + \begin{bmatrix} 0 \\ 0 \\ 0 \\ \frac{K_2}{M_2} \end{bmatrix} \cdot \left[\frac{dz_p}{dt} \right] \tag{0-1}$$

where: K_1 = spring stiffness [N/m],
C_1 = damper stiffness [Ns/m],
K_2 = tire stiffness [N/m],
M_1 = vehicle body mass [kg.],
M_2 = axle mass [kg.],
z_1 = vertical speed of vehicle mass [m/s],
z_2 = vertical speed of axle mass [m/s],
v_1 = vertical speed of vehicle body mass [m/s^2],
v_2 = vertical speed of axle mass [m/s^2].
z_p = elevation of the profile [mm],
t = the time that is needed for the vehicle to cover the distance between to measured points in the road profile [s]

For ease of notation, equation (0-1) will be simplified into the form of equation (0-2).

$$\frac{d[\bar{Z}]}{dt} = [\bar{A}]\cdot[\bar{Z}] + [\bar{B}]\cdot[\bar{Z}_p] \qquad (0\text{-}2)$$

The tire forces generated by the vehicle can now directly be determined from the values in the $\bar{Z}$ matrix. Before calculating the tire forces, the $\bar{Z}$ matrix has to be determined for all the point along the road. This is done using the method proposed by the World Bank, which was originally used to determine IRI values. The method is described in the following equations.

$$[ST] = [\bar{I}] + \frac{[\bar{A}]\cdot dt}{1!} + \frac{[\bar{A}]^2\,dt}{2!} + \frac{[\bar{A}]^n\,dt}{n!} + \ldots \qquad (0\text{-}3)$$

$$[\overline{RD}] = [\bar{A}]\cdot([ST] - [\bar{I}])\cdot[\bar{B}] \qquad (0\text{-}4)$$

$$[\bar{Z}] = [ST][\bar{Z}^*] + [\overline{RD}]\cdot[\bar{Z}p] \qquad (0\text{-}5)$$

The value of the "*new*" [Z] matrix is calculated from the values in the matrix at a previous point on the profile. The simulation is started by stating that the masses in the model do not have a vertical speed or acceleration. Solving differential equations requires the state of the system at a previous point in time.
Using the above-mentioned formulae it is now possible to calculate the vertical accelerations off both masses at each point along the road.
The resulting in- or decrease in the tire forces is then calculated using the following simple Newtonian law:

$$F_{tire} = m_1 \cdot a_1 + m_2 \cdot a_2 + g\cdot(m_1 + m_2) \qquad (\ 0\text{-}6)$$

Where F_{tire} = Force between tire and road [N],
M_1 = vehicle body mass [kg],
$M2$ = axle mass [kg],
a_1 = acceleration of the vehicle body [m/s^2]
a_2 = acceleration of the axle [m/s^2]
g = acceleration caused by the earth's gravity [9.8 m/s^2]

Modeling the vehicle and solving the necessary equations in only a part of the simulation. Finding the right parameters for the vehicle model is evenly important to the correctness of the simulation. That why the vehicle characteristics are taken of a actual two-axle truck (*see below*).

M_1	= 4,452	[kg],
M_2	= 650	[kg],
C_1	= 30,000	[Ns/m],
K_1	= 700,000	[N/m],
K_2	= 4,000,000	[N/m].
g	= 9.8	[m/s^2]

The mass of the vehicle body is chosen in such a way that the total wheel load is 50 [kN] which corresponds with an axle load of 100 [kN] (*10 tons*).

3.2 SimCar Vehicle Simulation Software

For the purpose of simulating a vehicle traveling over the road, a computer program was designed and programmed using a Fourth-Generation programming environment called Borland Delphi©. This visual programming environment that is based on Pascal object oriented programming language (*OOP*). Delphi© is called a visual programming enviremont as the elements that make up the user interface (*buttons, menus*) are already preprogrammed in the developers environment of Delphi. The programmer just adds the code that is initiated by "clicking" a button on the interface. The standard "*Tools*"-box of Delphi was extended by a matrix toolbox that was obtained from the Internet as a "*shareware*" product. This means that the programmer is only allowed to distribute programs that are developed using this tool if the programmer purchased the corresponding software license. This is not the case for CarSim and that is why the program can not be distributed as a fully functional software package. The resulting application is named SimCar and is still in the development stage. The current version of the program is version 0.15.

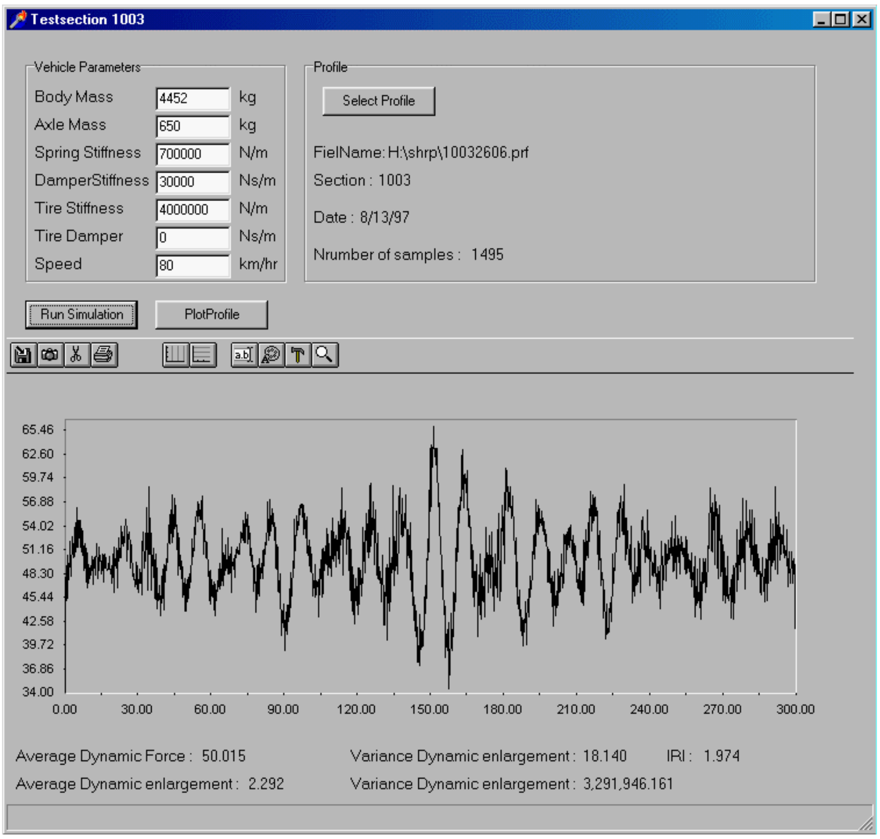

figure 0-2 Snapshot of SimCar version 0.15

The program enables the user to specify the road profile and the vehicle parameters needed to run the simulation successfully. The program then shows a plot of the tire force along the road. The results can be saved in tabular text files, which in it's turn can be imported in a so-called spread sheet program.

3.3 Applied Vehicle Simulations

The vehicle simulations are to be carried out on road profiles that are measured using the Dutch-ARAN. The simulations are done in two parts. The first part is to determine the effects of speed on the total vertical tire forces. The second part is to calculate the dynamic vehicle loading on all of the profiles in the sample.

3.3.1 Variation of vehicle speed

The maximum speed on the Dutch secondary roads is 80 [km/hr]. The average speed will therefore be about the same as the maximum speed with variation above and below the speed limit.
The effect of speed is examined by varying the simulation speed from 65 to 95 [km/hr.]. (0-3) shows the results of the simulation on a profile with an *IRI* of 1.75.

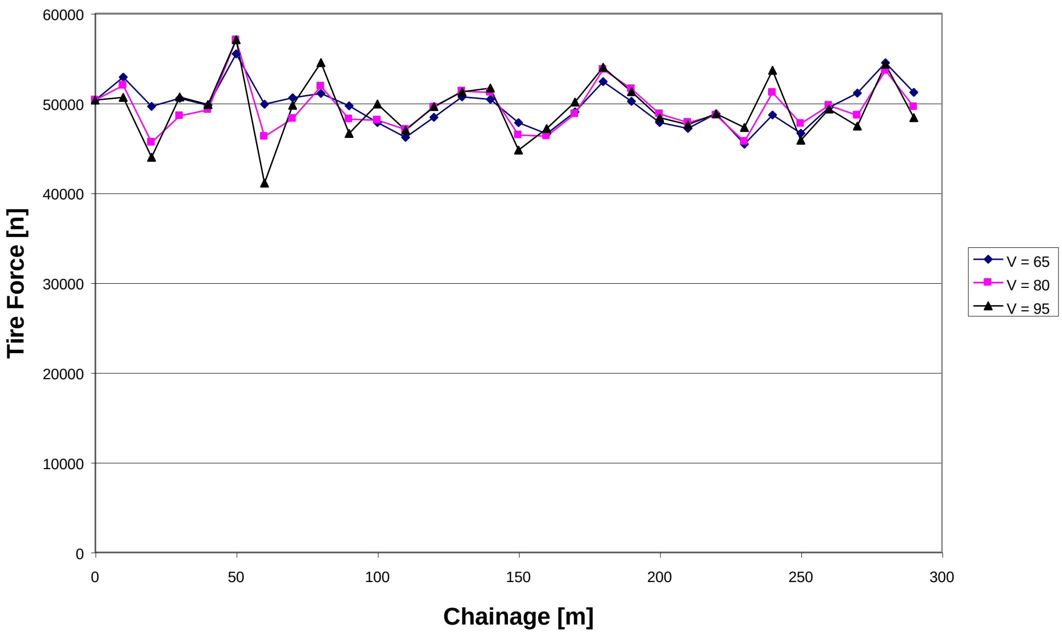

Figure 0-3 Simulations at different speeds

The conclusion that can be drawn from this simulation is that in- or decreasing the speed has a marginal effect on the dynamic tire forces (*see Table 0-1*).

Speed	65 [km/hr]	80 [km/hr]	95 [km/hr]
Average	49,681	49,439	49,411
Standard Deviation	2,303	2,605	3,374

Table 0-1 Speed Variations

3.3.2 Vehicle Simulations

The above-mentioned conclusion, that speed does not influence the absolute tire forces, has led to believe that simulating at one speed (*80 [km/hr.]*) is sufficient in this case. Simulations were done for all of the profiles of the sample. The following plots are of those profiles that cover the whole range of *IRI* values within the sample and thus give an overview of the vehicle reactions for the range of longitudinal unevenness in the sample. The dynamic enlargement in the figures is defined as the difference between the simulated tire force and the static tire force.

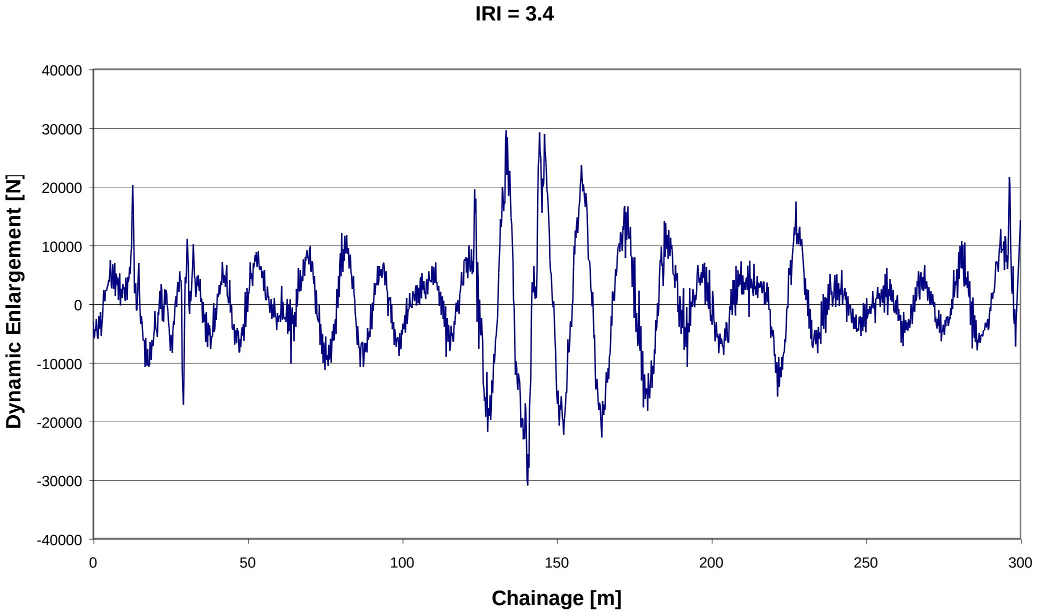

Figure 0-4 Dynamic enlargements of tire forces for an IRI of 3.4

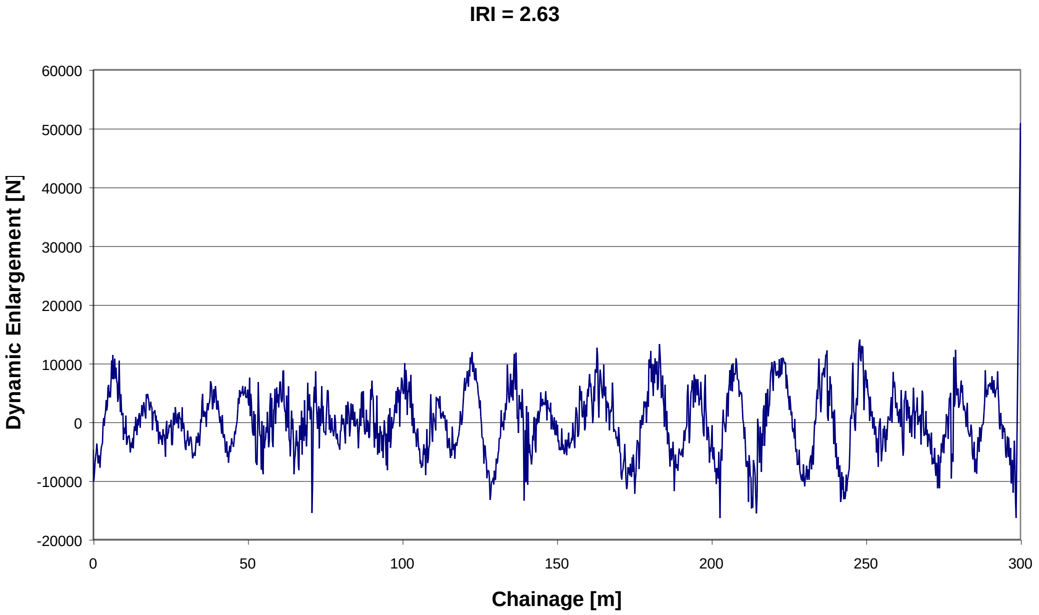

Figure 0-5 Dynamic enlargements of tire forces for an IRI of 2.63

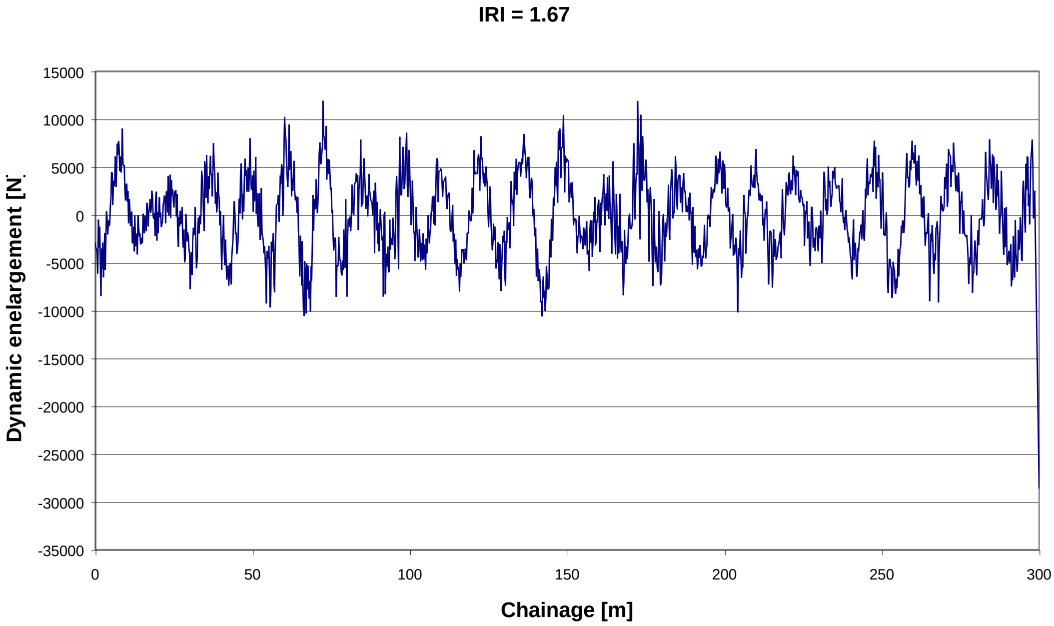

Figure 0-6 Dynamic enlargements of tire forces for an IRI of 1.67

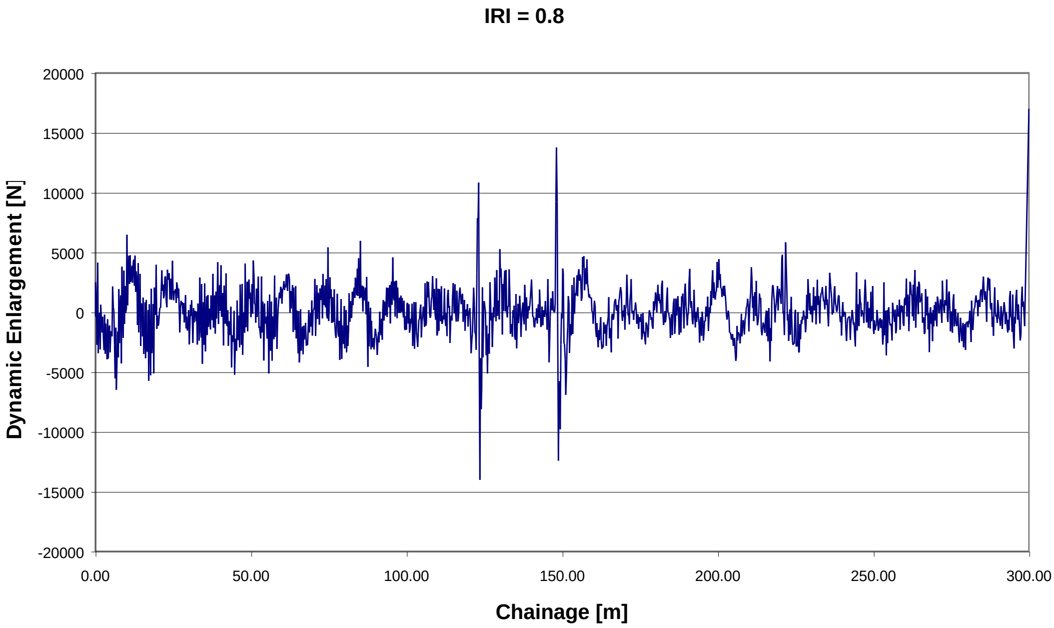

Figure 0-7 Dynamic enlargements of tire forces for an IRI of 0.8

The plots clearly show that a decrease in the pavement's roughness will result in smaller variation in the dynamic enlargement. A point of interest is the plot from Figure 0-4, which show an area along the road in which the vehicle is tuned in to it's "*eigen-frequentie*". A second observation that is made from the simulations is that the average dynamic enlargement is 0. In other words, the dynamic forces do not result in an increase of the average tire forces. This made it necessary to quantify the dynamic loading not by the average tire forces but by the variation in the dynamic enlargement. The standard deviation of the dynamic enlargement is chosen to serve this purpose.

The standard deviation of the dynamic tire forces is a good indicator for the forces that occur on a given profile. Adding the standard deviation to the average tire force will account for approximately 85[%] of the forces that occur on the pavement. Figure 0-8 shows the results for all the simulations that are done. The standard deviation shows a normal distribution with an average of 3.2[kN] and a standard deviation of 1.1[kN]. The results correspond well with the *IRI* distribution of the pavement.

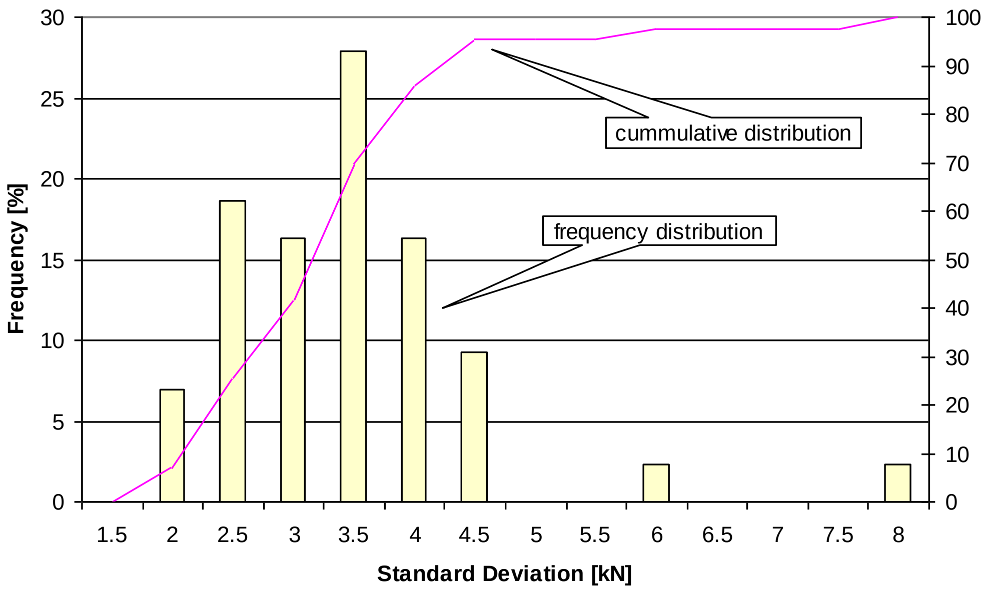

Figure 0-8 Standard deviations of the dynamic tire forces

The calculated standard deviations of the tire forces will be used in Chapter 4 to determine the influence of these variations on rutting.

3.4 Relationship between IRI and Dynamic Vehicle Loading

The actual simulation of the vehicle on a given road could prove to be difficult, or maybe even impossible, because of the lack of accurate profiles. Quantifying the dynamic tire forces using a simpler method could prove to be very useful in practice. A commonly used indicator for the longitudinal unevenness is the *IRI* (*see Appendix f*), which is an international standard to describe longitudinal unevenness. Since the *IRI* is calculated from the total movement of the spring suspension system, it can be expected that the *IRI* and the variation in tire forces are strongly correlated. Therefore a relationship was developed between the *IRI* and the variation in tire forces (*see* Figure 0-9). Observation of the plot makes it obvious that there is a good relationship between these two variables. Quantifying the relationship is done with the method of regression analysis and resulted in the relationship described in equation *(0-7)*.

$$SD_{force} = 2.25 \cdot IRI \tag{0-7}$$

Where: SD_{force} = standard deviation of the tire forces [kN],
IRI = (I)nternational (R)oughness (I)ndex.

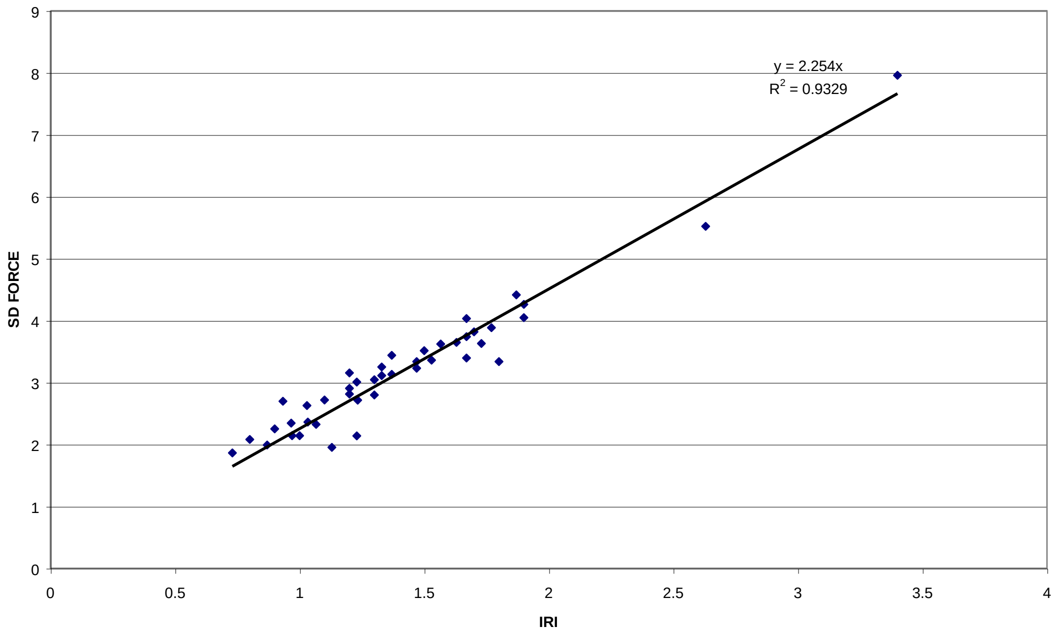

Figure 0-9 Relationships between IRI and the Variation in dynamic loading

3.5 Conclusions

The following conclusions can be drawn from the vehicle simulations:

1. Variation of the vehicle speed has only a marginal influence on the total tire load (*in this sample*),
2. The *IRI* is a good indicator for the variance in the dynamic tire loading,

CHAPTER 4 DESCRITION OF TEST-SECTIONS

This chapter will discuss the data that were used in this study. The object is to give the reader an overview of the available data and methods that are used to obtain these data. This is preliminary overview and contains al the available data on the secondary roads that are monitors in the SHRP-NL project.

4.1 A brief Introduction into the SHRP-NL project

The Strategic Highway Research Program is a large-scale project for monitoring long-term pavement performance (*LTPP*) that originated in the United States of America in 1989. The Dutch road authorities were quick to realize the potential of such a program in the development of pavement performance models, keeping in mind the success of the American association of State highway and Transpiration Officials (*AASHO*) full scale tests of the late 50's. That is why the Dutch version of the project was started in 1990 as a downscaled version of the American project. The Dutch version of the program, called SHRP-NL, differs from the other international version of *SHRP* in the fact that the project is not only intended as a mean of translating the SHRP-USA findings to Dutch circumstances but to come up with new pavement performance models of their own.
The project group was established in 1990, and was made responsible for the daily management of the project. The project group is situated in the building of the Road and Hydraulic Engineering Department of the Dutch Ministry of Transport, Public Works and Water Management (*RHED*) in the city of Delft.

4.2 Selection of SHRP-NL Test Sections

The criteria for the selection of the test-sections are divided in criteria that are used by the project group and one criterion that is used specifically for this study.

4.2.1 The SHRP-NL selection criteria

The SHRP-NL data set contains a total of 240 test sections which are divided into two groups, namely a group of 144 sections that are used to develop pavement performance models and a group of 96 sections to study the effects of maintenance. The SHRP-NL group used a number of criteria that are used in the selection of the test sections.

1. The pavement has to have the same type of overlay along the whole section. In this way the variations can only be caused by the pavement structure and not by the pavement material.
2. No crossings, parking places and sharp curves are allowed within the sections.
3. The embankment, if any, should be constant over the whole length of section,
4. The section has to be free of local repairs,

5. It has to be possible the close of the section for traffic. This criterion is necessary as it is quite impossible to do frequent measurement while the road is open to normal traffic.
6. The section should not have any local widening of the traffic lane,
7. The pavement structure should be homogeneous along the section.

These criteria are necessary to make sure that the incidental abnormalities do not determine the overall trends in the database. An example of such abnormalities is a test-section that has a bridge in the middle of the section. This would cause the *IRI* (*see Appendix A*) value to increase. The increase is a coincident that effects the overall view of the road and therefore should be avoided.
The test-sections that comply with the criteria 1 through 6 are offered to the SHRP-NL team by the governing road authorities. Criterion number seven is checked by using a Lacroix Defelctograph (*see paragraph 4.3.2*). The deflection of the pavement structure is measured at several locations along the pavement, producing the deflection profile shown in Figure 0-1.

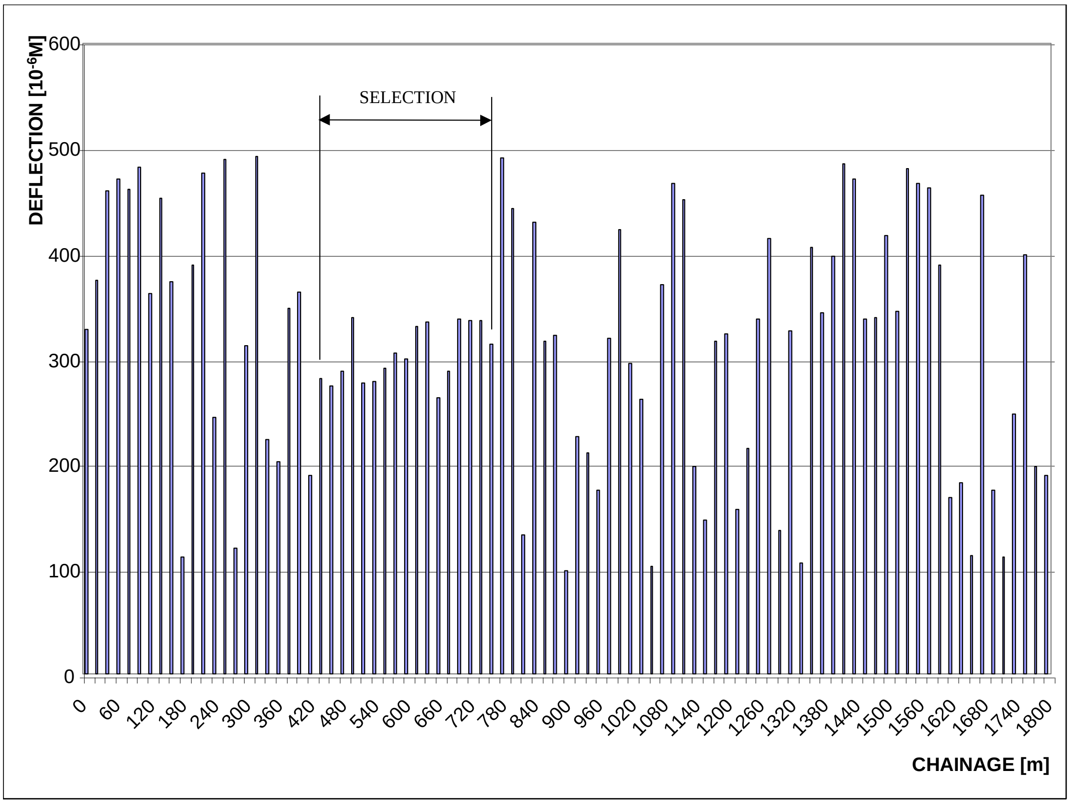

Figure 0-1 Deflection profile

The resulting test section is chosen in that area where the deflection profile shows the least variation. The result of the selection criteria is a data set of test sections that do not contain any local abnormalities.

4.2.2 Selection criterion used In this study

One more selection criterion is used in this study namely: the use of only secondary roads. This means that the highways, urban and farm to market roads are removed from the data set. There are two reasons for eliminating these roads. Highways are excluded, mainly to limit the number of entries into the data set. The farm to market and urban roads are excluded from the data sets because the longitudinal profiles of these roads are missing as the speed at which these roads can be measured is below the minimum speed required by the ARAN. The implementation of this criterion decreased the number of test-section to 40 (*see appendix for C overview of the test-sections*).

4.3 Description of test sections

Figure 4-2 shows an overview of a standard SHRP-NL test section. Every test section is 300m long with two reserved areas of 25m at the beginning and the end of the test section that are used to drill core samples of the pavement structure making the total length of 350m. The length of the section is chosen in such a way that the sections are long enough to do some actual measurements, while keeping the section short enough not to introduce irregularities in the pavement structure. The figure also shows the location where of the FWD measurements and core samples are taken.

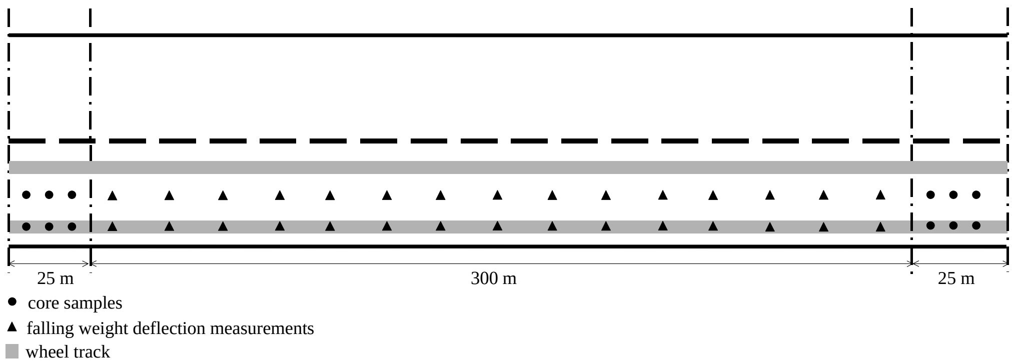

Figure 0-2 SHRP-NL test section

Inspection teams do rut-depth measurements at 10m intervals all along the test-section. The sections are also marked by special markers (*see Figure 4-3*) to insure that the right section and lane are inspected.

Figure 0-3 SHRP-NL marking

The test-sections are indexed using an SHRP-ID number. This ID consists of four numbers and is unique for each test-section.

4.4 Preliminary Measurements

The data in the data set of SHRP-NL is divided in measurements that occur once, at the start of the program and reoccurring measurements. The preliminary measured variables are considered to be constant for the whole life span of the pavement structure. The following paragraphs will discuss these "*one-time-only*" measurements for the 40 sections that are used in this study.

4.4.1 Layer Thickness

Core samples are taken at the beginning and end of each section to measure the actual thickness of each of the layers that make up the pavement structure. A total of twelve core samples are taken from each section. The layer thickness that is entered into the database is the average of the twelve samples. The following figure gives the frequency distribution of the asphalt thickness used in this study.

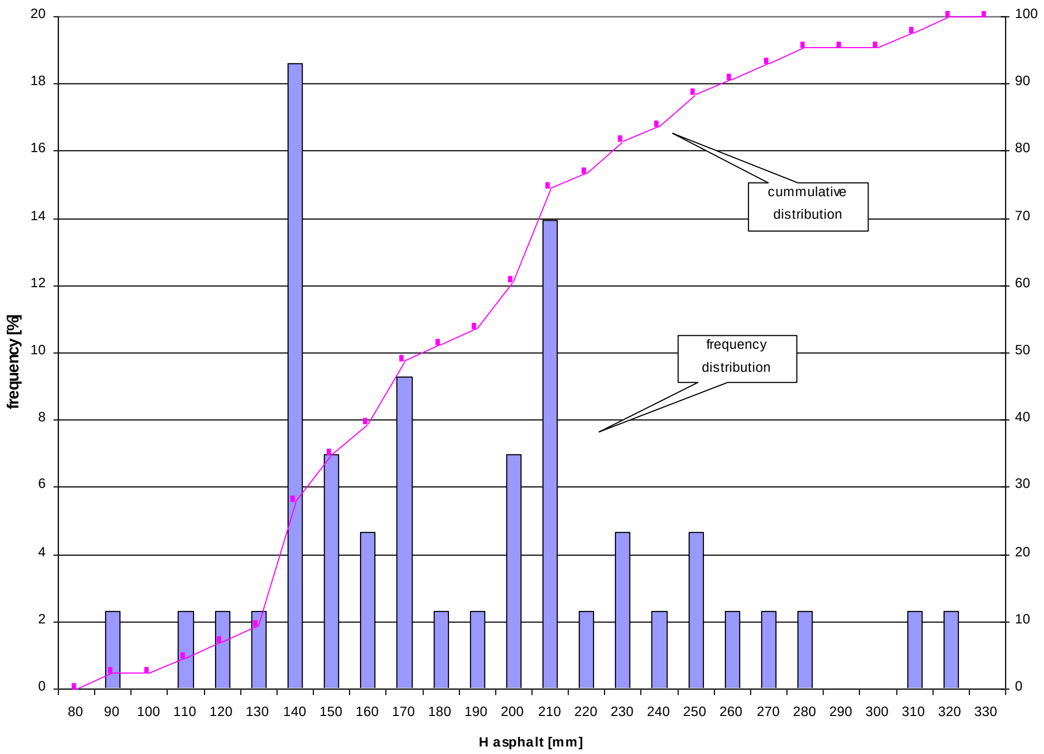

Figure 0-4 frequency distribution of asphalt layer thickness

The figure clearly shows a great diversity in the asphalt layer thickness with layers of 140 and 210[mm] prevailing over the rest. The base thickness and type are also entered into the SHRP-NL database. Figure 4-5 is compilation of the different layers specified per base type.

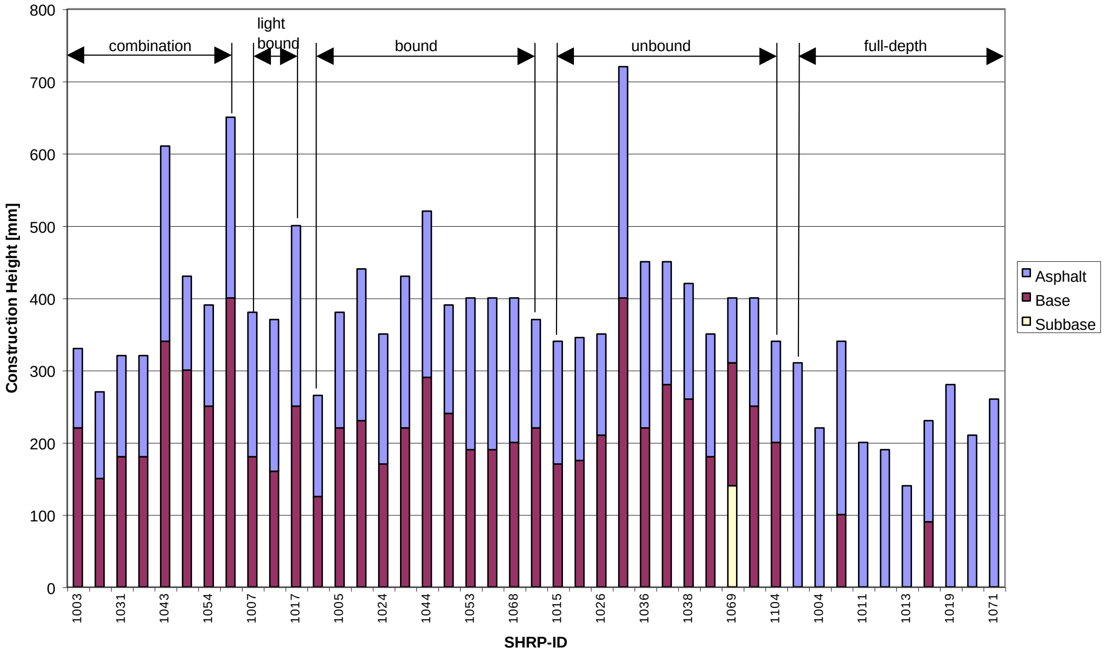

Figure 0-5 Construction Heights

Combination bases are bases that are made of light-bound, unbound and bound base materials. The full-depth asphalt constructions also include those pavements that use a sand-asphalt base materials.

4.4.2 Overlay Age

This study is focused on the way rut develops. That in this research the last date of overlay is taken as the reference for the time it took to develop the measured rut-depth. The road authorities provided the latest date of overlay.

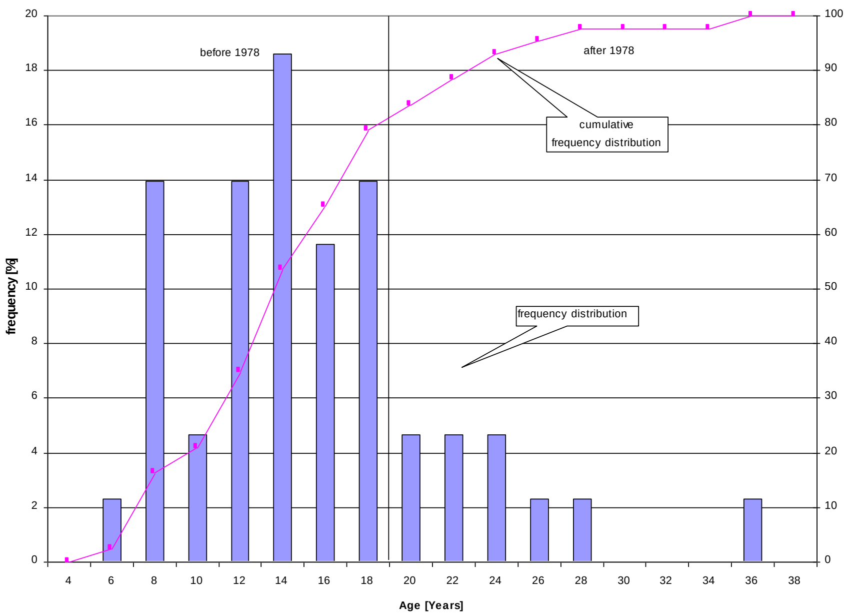

Figure 0-6 Frequency distribution of overlay age

The frequency distribution suggests that the overlay age is distributed normally within the SHRP-NL database. The test section with the overlay age of 36 years is obviously what is referred to as an "*outlier*" meaning that this section is not representative of the whole sample. Another observation can be made from the figure is that the average overlay age is about 14 [years] with a standard deviation of 5 [years] (*these numbers are calculated without the 36 year old pavement*).

4.4.3 Traffic

The traffic loading at the SHRP-NL sections is also measured at one time during the program. The governing road authorities did these measurements themselves. The intensities are measures at different times, which makes it necessary to correct the data set values to represent intensities of 1996 (*This is the year in which the visual inspections were done that are used in this study*). The correction is done using equation (4-1).

$$I_{96} = I_t \cdot (1 + \frac{G}{100})^{96-t} \qquad \textit{(0-1)}$$

where: I_{96} = the traffic intensity in 1996,
I_t = traffic intensity at time of measurement,
G = growth rate [%],
T = year of measurement.

The resulting corrected traffic intensities are shown in Figure 4-7.

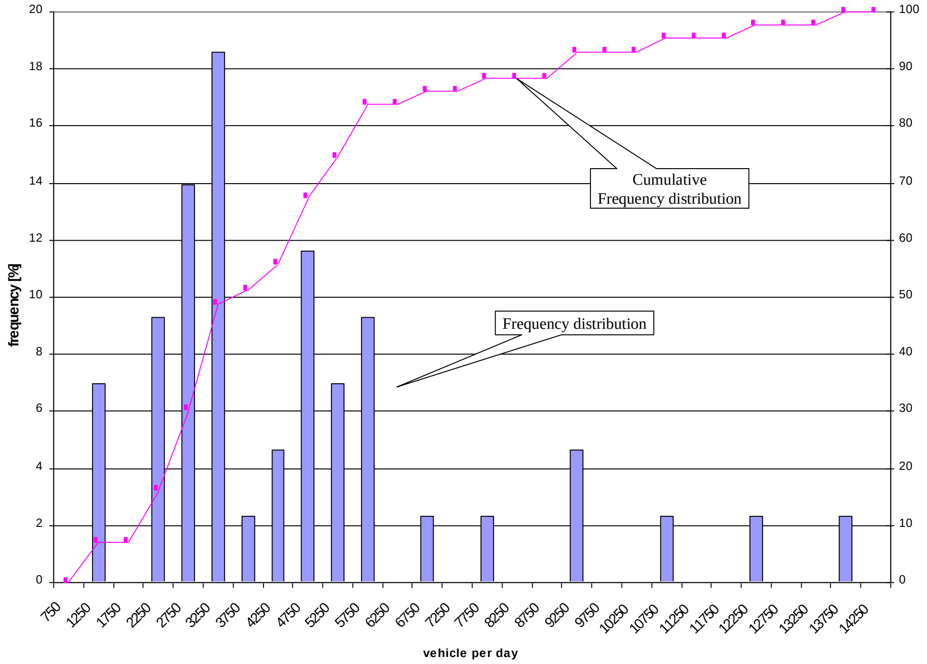

Figure 0-7 Frequency distribution of Traffic Intensity ('96)

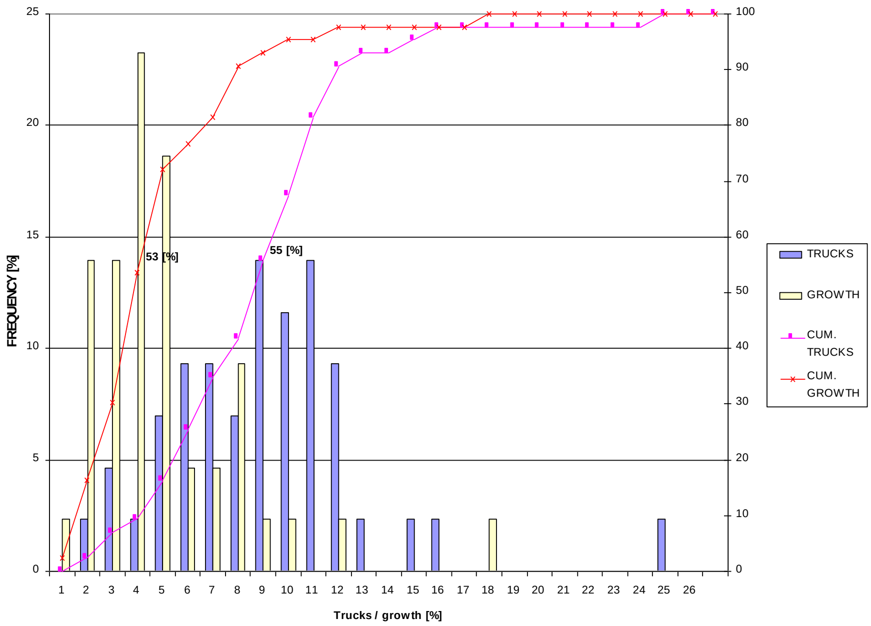

Figure 0-8 Frequency distribution of both truck and growth percentage

Figure 4-8 shows the frequency distribution of both truck percentage and the growth rate. Both values correspond well with values that are found on typical Dutch roads. The traffic growth has an average of 4[%] and the average percentage of trucks is 9[%].

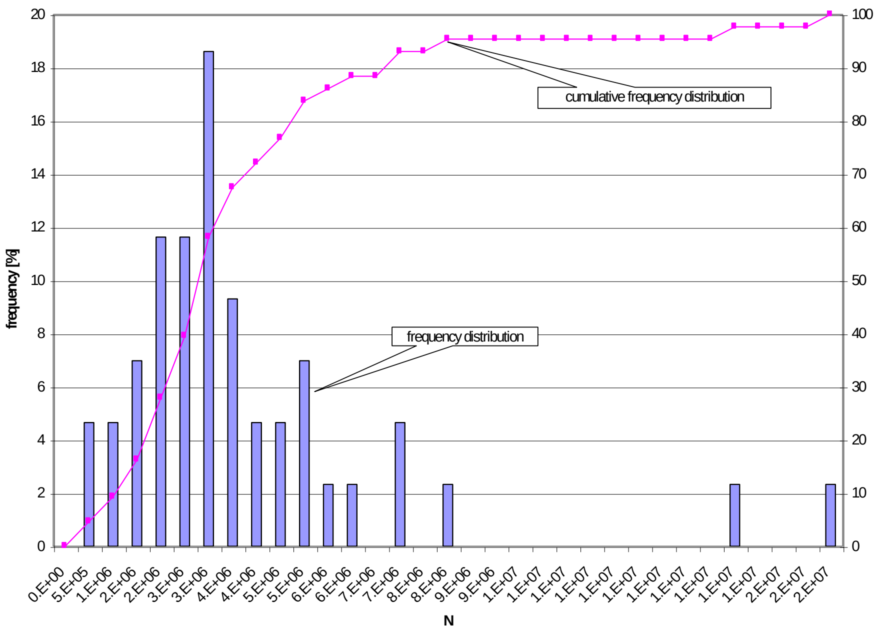

Figure 0-9 Frequency Distribution of number of vehicle passages

Figure 4-9 represents the number of equivalent 100[kN] axle loads, which is the result of combining the overlay age, the percentage trucks, the traffic intensities and the growth rate of the traffic. *N* is calculated using the equation from the RHED pavement design manual [7].

$$N_{eq} = V \cdot W \cdot F_r \cdot F_s \cdot D_v \cdot F_a \cdot F_b \cdot \frac{\left(1+\frac{G}{100}\right)^L - 1}{\frac{G}{100}} \qquad (0\text{-}2)$$

where: V = Number of trucks per direction,
W = number of workday per year [days],
F_r = correction for the number of lanes per direction,
F_s = correction for the width of the lane,
D_v = Truck damage factor,
F_a = correction factor for the increase in axle loads,
F_b = correction factor for the use of "*super-singles*",
G = annual traffic growth rate [%],
L = age of pavement [years].

Number of workdays per year
The number of workdays is estimated to be 250 days per year. This number is valid for roads that are open to traffic for the whole year.

Correction factor for the number of lanes per direction
If a road has more then one lane per direction, the number of truck passages will be distributed between all these lanes. This causes a reduction of in the number of trucks that will use the right lane. The reduction is dependent on the number of lanes per direction. Most of the 40 test section that are used, consist of only one lane per direction, there will be no need for reduction and Fr = 1.0.

Correction factor for the width of the lane
Not all the vehicles travel over the same line on a road. The transverse positions of the tire show a variance. This also reduces the number of vehicle passages. The reduction is dependent on the width of the lane. As all the roads in that are evaluated in this research program are of the same category (secondary roads), it is assumed that the roads all have the same width of 3.2 [m]. F_s = 1.07.

Truck damage factor
The truck damage factor is defined as the number of standard axle loads per truck. As the distribution is unknown for the secondary roads that are used in this study, the value was estimated by using table 3 on page 5-5 of the RHED road design manual [7].

Number of trucks per day per direction	Truck Damage Factor
< 1000	0.9
1000 - 3000	1.2
> 3000	1.3

Table 0-1 truck damage factor

Correction factor for the increase in axle loads
As the Dutch guidelines into the maximum axle loads are changed in order to comply with the E.E.C guidelines, the maximum axle load will be increased to 110 [kN]. Although the new guidelines are net yet in effect in the Netherlands, it is assumed that an increase in axle loads has already occurred. This has led to the correction factor of 1.1.

Super Single correction factor
Recent years have shown an increase in the use of the so-called "*super-single*" tires. The super-single tire has a smaller contact area between the tire and the road then the total contact area of a dual wheel configuration carrying the same load. This means that the super single will lead to accelerated road wear. The super-single correction factor was introduced to counter this effect. The use of the "*super-single*" is taken into account with a super-single correction factor of 1.05.

Traffic growth factor
Although the values were obtained on different dates, it is assumed that the growth is constant through the lifetime of the construction.

Age of construction
The date of the last overlay has been chosen as the age of the construction. As rutting is the only form of damage that will be evaluated in this research project and rutting is primarily a result of deformation in the asphalt-layer, this is a reasonable assumption. The last date of overlay is also provided by the SHRP-NL database.

4.3 Annual Measurements

The SHRP-NL program was designed to create pavement performance models. This meant that the damage (*both visible and invisible*) had to be monitored on a regular basis. Following the damage accumulation in time makes it possible to develop models that can predict pavement deterioration in time. Four types of measurements are done each year. The following paragraphs will discuss each of these measurements.

4.3.1 ARAN profile measurements

The ARAN, which stands for Automated Road Analyzer, can be described as a multi-functional measuring vehicle capable of doing a wide variety of road measurements in one single pass, such as measuring the transverse and longitudinal profiles and making video recordings of the road. The ARAN is capable of doing these measurements at speeds varying from 40 – 90 [km/hr.].

Longitudinal profile
The ARAN is equipped with two accelerometers that constantly measure the vertical accelerations of both the vehicle body and axle (*see figure 0-10*). The road profile is back calculated by a double integration of the acceleration profile. In other words:

The road profile is measured by calculating the movement of the axle in reference to the ARAN's chassis. The height if the chassis is determined by the accelerometer that is fixed to the chassis.

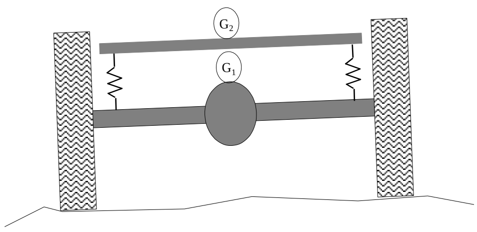

figure 0-10 ARAN accelerometers

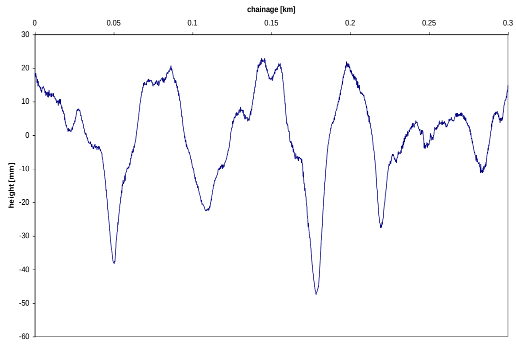

figure 0-11 Sample longitudinal profile

Only the measured profile of the ARAN is of interest in this study, as rut-depth measurements are obtained from the visual inspections. the longitudinal unevenness of the road profiles is translated to the International Roughness Index and entered into the SHRP-NL database.

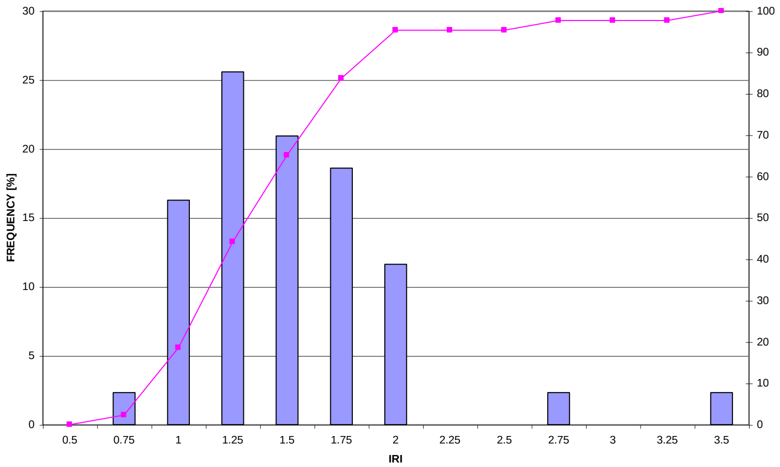

Figure 0-12 frequency distribution of IRI

Figure 4-13 shows the distribution of the IRI values from the 40 test-sections in this study. The values that are represented are the average *IRI* values of the 300m test sections. The distribution clearly shows a normal distribution within the *IRI* values with two distinct "*outliers*" at *IRI* values of 2.63 and 3.4. The figure also shows that the majority of the *IRI* values lie between 1 and 2. In short, the *IRI* values suggest that the roads in this data set are very smooth with a minimal variation between the different test-sections.

4.3.2 Falling Weight Deflectometer (FWD)

The falling weight deflectometer is considered to be an ideal tool for determining the pavement's stiffness properties. The FWD simulates a vehicle load of 50[kN] and registers the deflection in the pavement resulting from the load. The layer stiffness can then be back calculated from the deflection bowl of the FWD. It is for this reason that the SHRP-NL project incorporated FWD measurements in the annual inspections. SHRP-NL the use of the Dynatest 8000, which is also used in the North American version of the research program. The advantage of using the same device is the possibility of a direct comparison between the American and Dutch measurements.

The procedure called for measurements between the wheel tracks and in the right wheel-track. This procedure should provide information on the deterioration of the pavement structure by comparing new material (*material between the wheel-tracks*) with material that has been in service for a while (*the right wheel-track*). The deflection measurements are also done with three different loads (*25, 50, 75 [kN]*) and the asphalt temperature is measured at three different locations in the asphalt layer.
Three different deflection parameters are included in the SHRP-NL database namely;

1. D_0, this is the deflection right under the falling weight. D_0 is considered to be indicative of the total bending stiffness of the pavement structure[5].
2. SCI_{300}, which is the difference between the measured deflection of D_0 and the deflection that is measured at 300[mm] from the center of the falling weight. SCI_{300} is considered as being indicative of the stiffness of the top layer [5].
3. SCI_{600}, is the difference between the deflection right under the falling weight and the deflection that is measured at a distance of 600[mm] from the center of the falling weight. SCI_{600} is considered as an indication for the stiffness of the base material[5].

As is mentioned above, the asphalt temperature is also measured during the FWD measurements. This is done in order to correct the measurements to one single temperature, to account for the temperature dependency of the asphaltic material. The stiffness of the asphaltic material is dependent on the temperature at which the measurements are done. The correction of the deflection values is done using equation (4-3) [5].

$$TNF = 1 + \left(a_1 + \frac{a_2}{h_1}\right)(T_A - 20) + \left(a_3 + \frac{a_4}{h_1}\right)(T_A - 20)^2 \qquad (0\text{-}3)$$

where: TNF = temperature normalization factor,
T_A = Asphalt temperature [°C],
h_1 = thickness of the asphalt layer [mm].

Variable	a_1 [°C^{-1}]	a_2 [mm/°C]	a_3 [0.001 °C^{-1}]	a_4 [mm/°C]
D_0	0.01661	-0.67095	0.28612	-0.01408
SCI_{225}	0.05955	-2.73223	1.48011	-0.08171
SCI_{300}	0.05398	-2.61130	1.28439	-0.07493
SCI_{450}	0.04720	-2.39175	1.05022	-0.06371
SCI_{600}	0.04190	-2.15168	0.87228	-0.05301

Table 0-2 Coefficients of tempreture normalization of FWD Deflections

The results of the temperature corrections are deflection values that can be directly compared to each other. As mentioned before, the deflection measurements are also done at different load levels. The measurements are therefore also corrected to one load level of 50[kN] (*contact pressure of 0.77[Mpa]*).

Figure 4-15 shows the frequency distribution of the corrected D_0. The plot indicates that the deflection has a more or less normal distribution with an average of 275[μm].

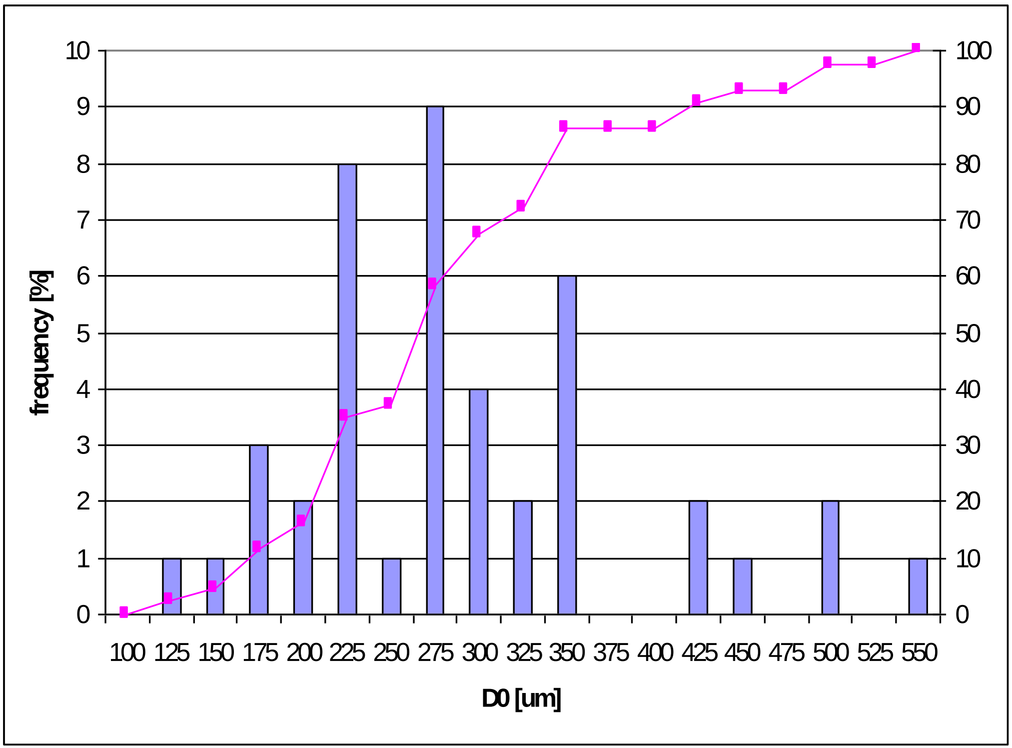

Figure 0-13 frequency distribution of D_0

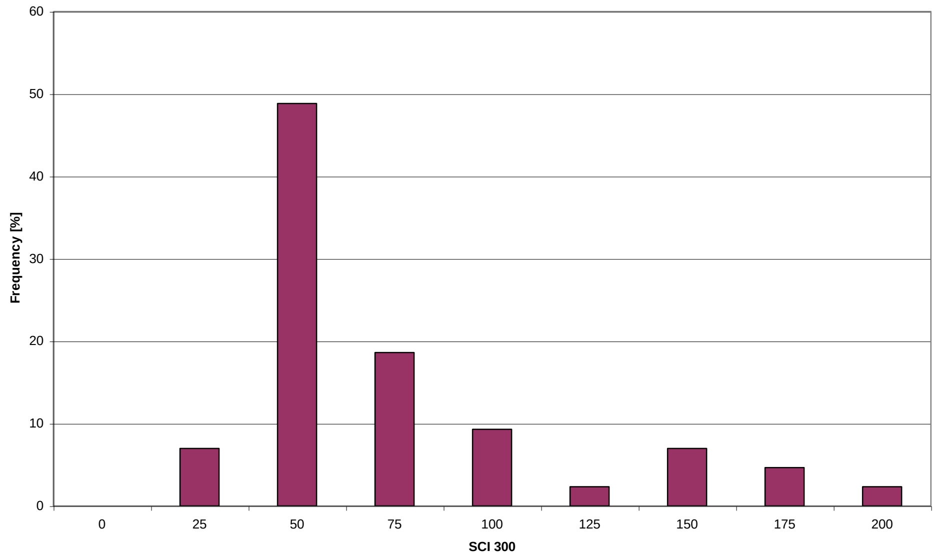

Figure 0-14

Frequency distribution of SCI_{300}

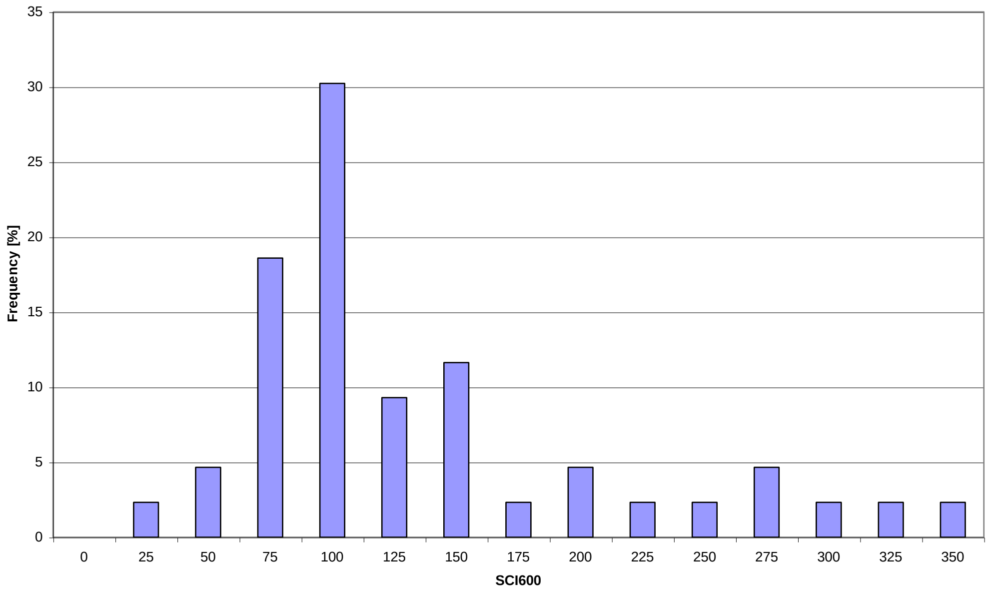

Figure 0-15 Frequency Distribution of SCI_{600}

Figure 4-14 and Figure 0-15 show the frequency distribution of both SCI_{300} and SCI_{600}. The distributions seem to have a more or less Poisson distribution.

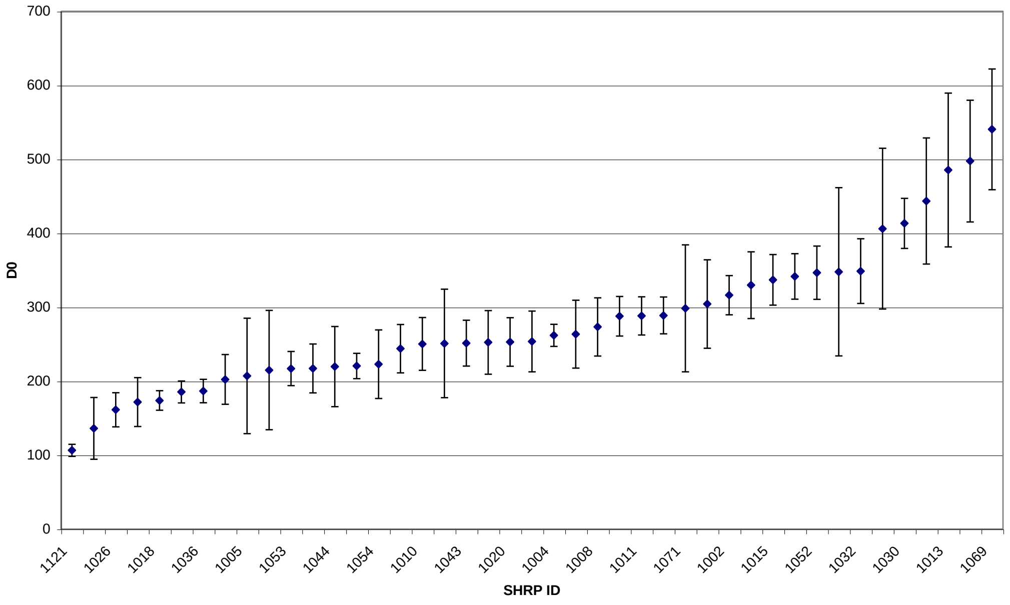

Figure 0-16 D_0 and the variation

Figure 0-16 shows the D_0 values sorted from in ascending order. The bars in the figure have length of the standard deviation of the deflection. The plot shows that, except for the large values if D_0, the standard deviation seems to vary only a small amount. This is the result of the selection criteria applied by SHRP-NL that states that the sections should be as homogeneous as possible (*see chapter 4.2*).

4.3.3 Visual Inspections

Visual inspections are done on all the test-sections that are included in the SHRP-NL date base. A number of different damage types are measured and registered on inspection forms (*see appendix d*). The description of the visual inspections will only include the rut-depth measurements, as these are the only measurements used in this study. Rut-depth measurements are done using the method prescribed by the R.H.E.D. using a 1.2[m] rod (*see Figure 0-17*). The rut-depth is defined as the maximum difference in elevation between the rod and the pavement.

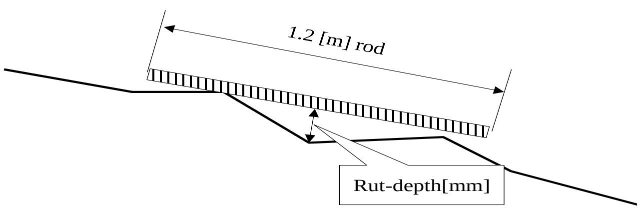

Figure 0-17 Rut-depth measurements

Rut-depth measurements are done every 10m and are later translated into an average rut-depth per 100m. This is done for both the left and the right wheel track. Figure 0-18 shows the distribution of the rut-depth of the 40 test-sections that are used in this study. The values that are represented here are the average rut-depth of both the left and right wheel tracks.

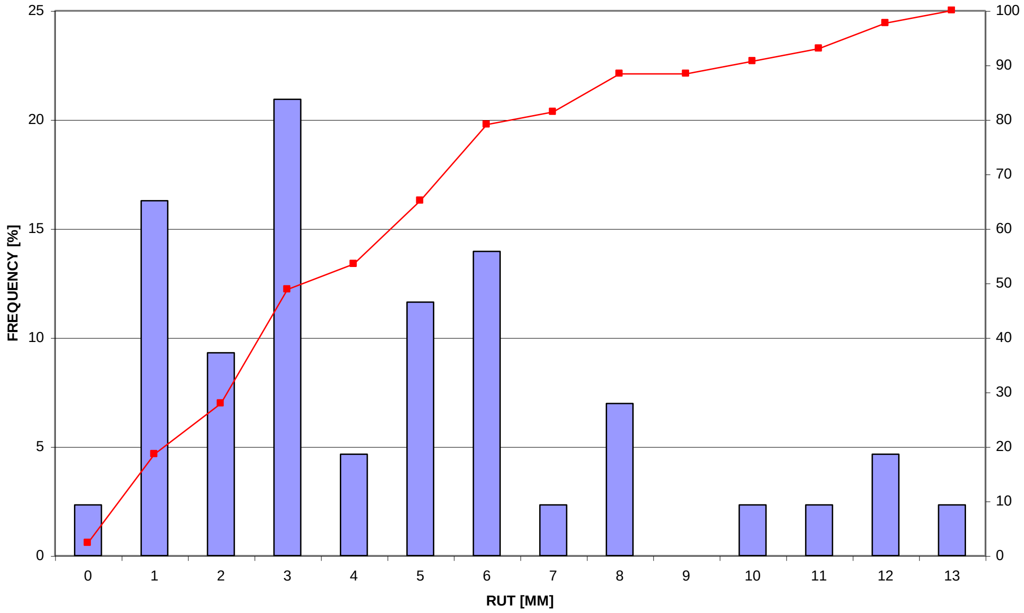

Figure 0-18 frequency distribution of rut

Figure 0-19 and Figure 0-20 show the distribution of rut within the test sections themselves. Observing figure 4-19 it becomes obvious that the rut within the sections can either have a Poisson or normal distribution. A second observation that can be made is that, although the test-section should be homogenous, some test sections develop a rut-depth profile that suggest otherwise.

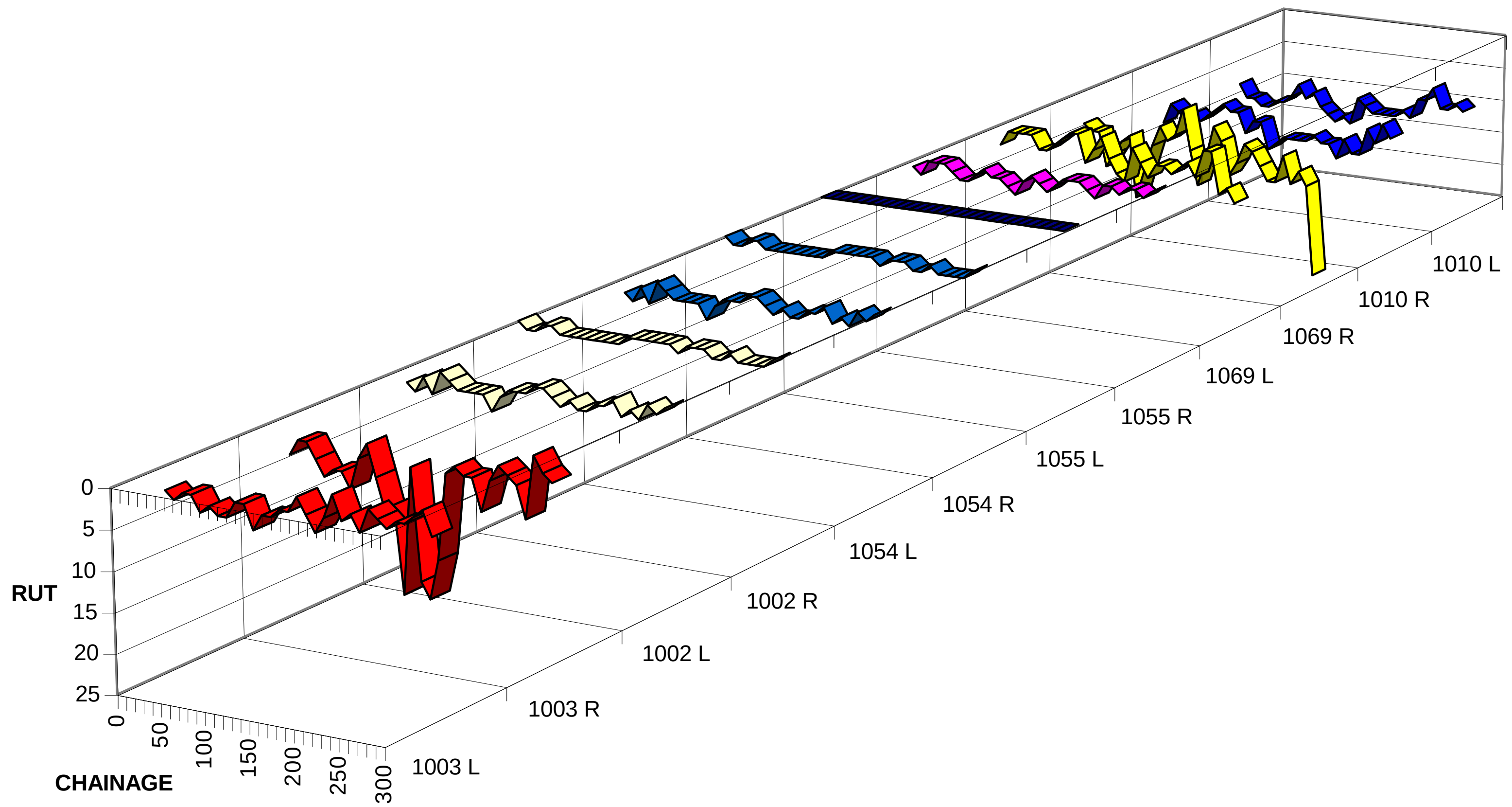

Figure 0-19 rut depths along pavement

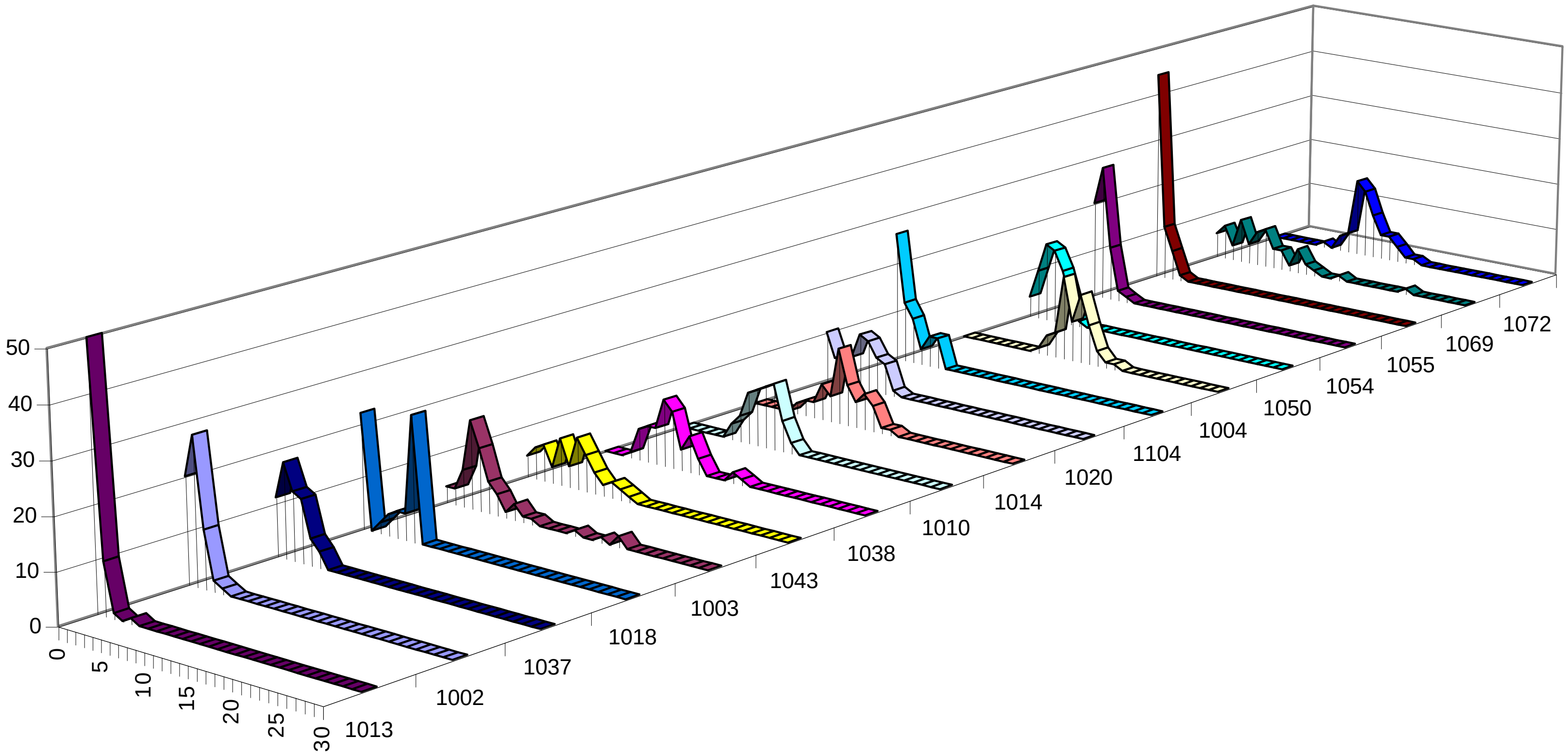

Figure 0-20 rut depth distributions within test section

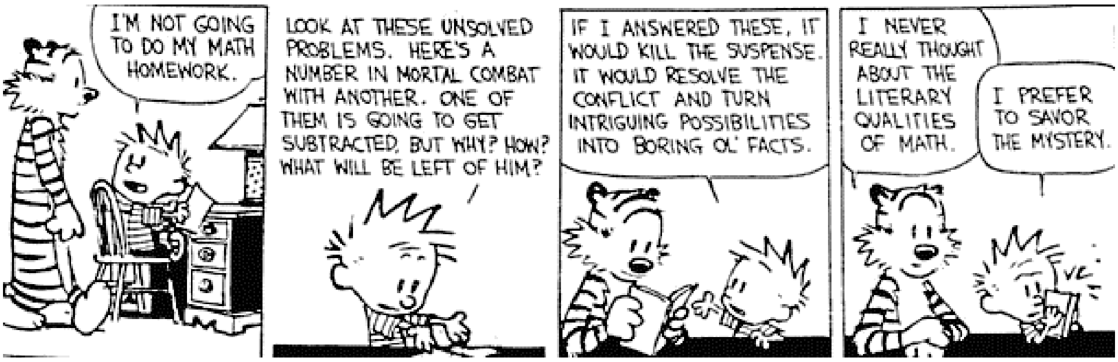

Bill Waterson 1987

CHAPTER 5 RUT-DEPTH PREDICTION MODEL

This chapter will deal with the development of rut development model using the method of regression analysis. The first step in developing such a model is to establish the necessary variables that help to explain rutting. As has been mentioned in the introduction of this report, the objective of this study is to determine the effect of dynamic vehicle loading, that is why dynamic vehicle loading is also added to the model. The second step is to determine the test sections that are eligible for use in the regression analysis and the third step is to determine the regression model and the values of its parameters. All the above mentioned steps will be described in this chapter and finally the model will be evaluated to examine its physical correctness.

5.1 Rut Model Variables

Mechanistic asphalt pavement rutting models use the following general relation. The relation describes rut-depth as a function of both the material and loading properties of the pavement structure.

$$u_p = a \cdot N^b$$

where u_p = permanent deformation of the pavement structure,
N = number of load repetitions,
a, b = material constants that describe the material characteristics and the stress conditions in the pavement structure.

The proposed alternations to the model are made in the reevaluation of the vehicle loading. As mentioned in the introduction of this report, the effects of the dynamic vehicle loading are to be studied by developing a regression model that incorporates a non-static approach to vehicle loading. 0 has already researched the reaction of vehicles to unevenness of the pavement and a model that relates the variation in vehicle loading to the commonly available *IRI* (*international roughness index*) value of the pavement. Both the number of vehicle passages and the standard deviation of the axle load (SD_{force}) will therefore be used to describe the total loading of the

pavement. The SD_{force} value is raised to the fourth power to take into account the extra damage that is done according to the "*fourth-power-law*[1]". Raising the SD_{force} to the fourth power is only an estimation of the extra damage caused by an increase in axle loads. The relationship between axle loads and damage was originally designed to review the decrease of the Present Serviceability Index that represents a combination of different damage types. The actual relationship between the increase in axle loads and rutting was never established in the AASHTO road test.
The other variables that are needed to complete the model are the ones that describe the material properties and the stress conditions. The SHRP-NL database has a number of entries that can be used to serve this purpose namely the deflection values and their derivatives and the thickness of the layers that are used in the pavement structure. The following paragraph will discuss the different variables that are available and which are finally chosen in for the purpose of modeling rutting.

5.1.1 Material properties

The material variables *a* and *b* are dependent on the material characteristics and the stress conditions in the pavement structure. As the data set does not contain actual entries for the pavement material characteristics (*see chapter 3*), alternative variables have to be sought that are able to serve this purpose. A number of variables from the data set can be used in the model as material parameters namely D_0, SCI_{300} and $H_{asphalt}$.
D_0 is considers as being indicative of the stiffness of the whole pavement structure while SCI_{300} gives an indication of the asphalt stiffness. $H_{asphalt}$ in combination with SCI_{300} can be used to describe the stress conditions in the asphalt layer. This makes a total of five possible variables that can be used to model the rut development. Preliminary regression analysis have indicates that some of these variables are not statistically significant to the regression models. The conclusion is that more then one of the variables can be excluded from the model and thus a further investigation of the variables seems inevitable. Low confidence levels of the regression parameter suggest that the variables could be dependent of each other. This dependency among the explaining variable was investigated by plotting the variables against each other (*see Figure 0-1 to Figure 0-23*).

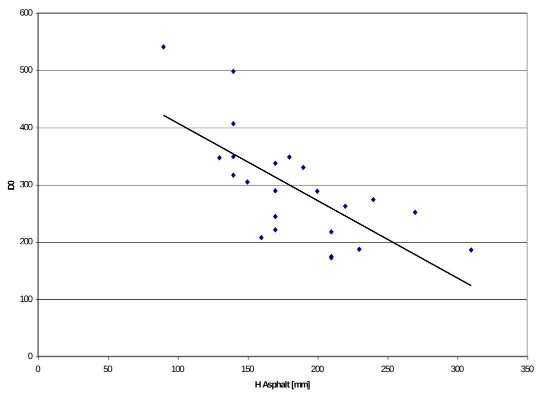

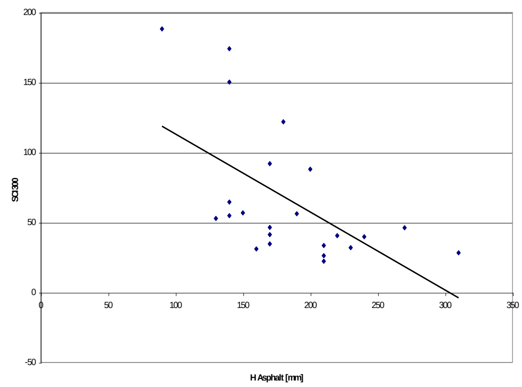

[1] The power of four results from full-scale pavement test carried out by the American Association of State and Highway Officials in Illinois. it was found from the tests that the decrease in pavement serviceability is inversely proportional to the axle load raised to the fourth power.

Figure 0-1 $H_{asphalt}$ versus D_0

Figure 0-2 $H_{asphalt}$ versus SCI_{300}

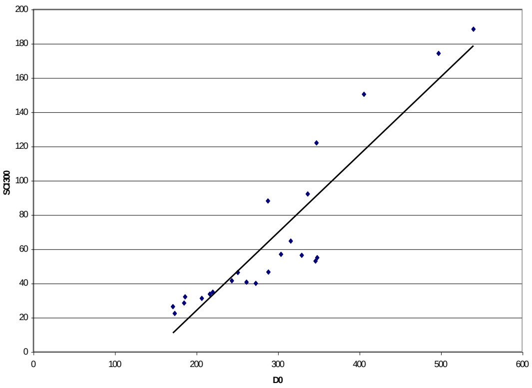

Figure 0-3 D_0 versus SCI_{300}

The dependency among the variables suggests that one variable only will be sufficiently adequate to describe both the material properties and the stress conditions in the pavement structure. D_0 is chosen as the variable that will be used in the further development of the rut depth model.

Previous research [11] has shown that the material properties of asphalt are not constant with time. Age is added to the model as an independent variable to take into account the changing of the asphalt material as a result of environmental influences. These influences are called "*aging*" that results in an increase of the stiffness of the asphalt mix and a decrease of the viscosity of the bitumen. The result of "*aging*" is an increase of the resistance of the asphalt material to rut development.

5.2 Rut-Depth Model

A total of four variables are used in the final model. Two variables are needed to describe the loading (N_{equ}, SD_{force}) of the pavement and two variables (D_0 *and Age*) explain the stress and material properties of the pavement.

A number of different regression models were fitted to the data set containing *N*, SD_{force}, D_0, and *Age*. The best fit to the data was obtained using the following regression model *(0-1)*.

$$RUT = \beta_1 \cdot \log(STDEV\_F^4) + \beta_2 \cdot \log(D_0) + \beta_3 \cdot \log(AGE) + \beta_4 \cdot \log(N) \qquad (0\text{-}1)$$

Where: *RUT* = rut [mm],

STDEF_F = standard deviation of the standard axle load [kN],

D_0 = the deflection measured under the falling weight [m^{-6}],

AGE = the age of the overlay [years]

N = the number of load repetitions.

Although the above mentioned regression did produce the best "*fit*" to the data samples, it did not produce a high accuracy. This meant that the data set had to be reexamined and an explanation had to be found for this low accuracy. The data set has to be examined for either data samples that indicate a different mechanism in the rut development or measurement errors. A total of three filters were applied to the data set that are able to produce a clean “*normalized*” set of test section.

5.2.1 Filter I, Age

Rut development on the Dutch roads became excessive after a few hot summers in the late 70’s. This is the reason that the mix specifications have changed since 1978 to increase the resistance to permanent deformation of the asphalt layer. The new mix specifications called for less bitumen to be used in the asphalt mix. The change in mix specification resulted in a different development of the rut-depth as a result of traffic loading. The applied filter to the variable *age* is therefore a very simple and straightforward one namely: “*Remove all those test-sections that have an asphalt overlay that was applied before 1978*”. The result of applying filter I is the elimination of 9 test-sections of the data set which leaves 31 entries.

5.2.2 Filter II, Rut Development

Another indication that the rut development shows a rather unusual behavior is the measured rut depth. Some road don not show any rutting even having been in service for some time (*section 1121 0 mm rut-depth, 6 years old*) while others show a remarkable low rut depth (*1013 shows less then a millimeter after being in service for 18 years*). This has led to the to the conclusion that some of the test sections will have to be excluded from the data set based on the rut development on that road. As the author had no means of establishing a guideline for what is reasonable, all the test sections that hat less then 1mm rut are to be excluded from the data set. 1mm was chosen as the rejection level because the rut measurements are only accurate to the nearest millimeter. This has led to the elimination of 6 test sections.

5.2.3 Filter III, Number of load repetitions

Another parameter that could indicate that the rut development mechanism would differ from the normal rut development, is the percentage of trucks on a particular test section. Test section 1054 has a very high percentage of trucks (*25%*). This is about twice the normal percentage that can be found on Dutch roads. The effect of such a high percentage is that the rut development is much stronger on this section if compared to the other normal sections. This has led to the elimination of test section 1054 from the data set. The last section to be eliminated from the data set is section 1072 that shows a remarkable high growth rate of 17.7 [%] per year. This is more then four times larger then the average rate of 4[%]. High growth rates are usually a temporary trend on a particular road. That is why section 1072 is also eliminated from the data set.

5.2.4 The second try

Running the regression analysis again of the remaining set of data samples did raise the accuracy of the model quit a bit. The R^2 of the model went up from 0.017 to 0.432

which means that now 43.2[%] of the variation of the model could be explained by this model. Although this is a significantly better result then before, the model is still not accurate enough to be considered a mean of predicting rutting.
Table 0-1 shows the result of the regression analysis using the mathematical model from equation *(0-1)*(*see appendix e for the interpretation of the regression results*)
The confidence levels that are mentioned in the table have to be added to the regression parameter value to obtain the confidence range of the mathematical model.

Variable	Value	68% (+/-)	90% (+/-)	95% (+/-)	99% (+/-)
β_1	0.577198	0.499562	0.822383	0.999124	1.286312
β_2	2.224882	1.039723	1.7116	2.079446	2.67716
β_3	-5.305977	2.233735	3.677192	4.46747	5.751597
β_4	0.547228	0.379598	0.624897	0.759196	0.977419

Table 0-1 Results of four-variable model

Further evaluation of the model is thus necessary in order to increase the accuracy.
The first step in the optimization of the mathematical model is the evaluation of the residual[2] plots.
Figure 4-4 shows the residuals for the different base materials that are used in the test-sections. The test-sections are divided in four classes that represent the materials that are used in the base of the pavement structure.
The residual plots show trends within each class of base types.

- The full-depth pavement structures tend to be <u>largely</u> over-estimated by the mathematical model,
- The bound based pavements show the tendency to be <u>greatly</u> underestimated by the model,
- The residuals of those sections that are built on unbound materials are also underestimated by the model, but the residuals are smaller (*the rut depth values are estimated more accurately*)
- The roads that are built using a combination of different base materials (*indicated by combination*) show a trend that can best be described as an average of the other types of bases.

[2] The residual of the regression analysis is the difference between the measured rut minus the predicted rut. The residual plot is a plot of the residual versus one of the variable.

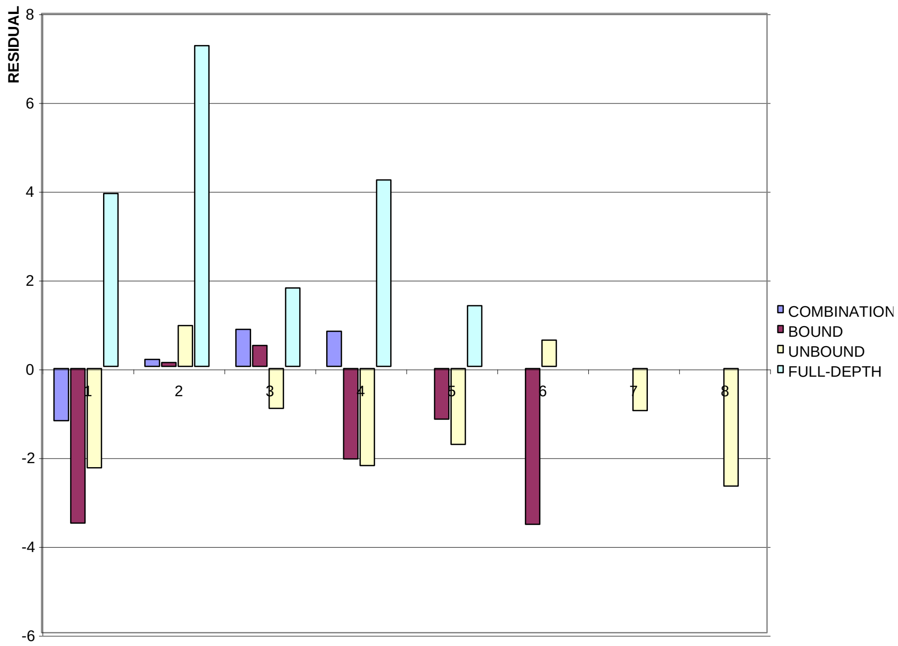

Figure 0-4 Residual plot per variable

The obvious trends in the residuals led to the introduction of the so-called dummy variables[3] [7], which make the model "*sensitive*" to the different types of base materials. The following dummy-variables are used to describe the different base types.

Base Type	Dummy Variable 1	Dummy Variable 2	Dummy Variable 3
Full Depth	10	1	10
Unbound	10	10	10
Bound	10	10	1
Combination	1	10	10

Table 0-2 Dummy variables

The mathematical model is now expanded to include seven variables instead of the earlier four (*see equation* (0-2)).

$$RUT = \beta_1 \cdot \log(STDEV\_F) + \beta_2 \cdot \log(D_0) + \beta_3 \cdot \log(AGE) + \beta_4 \cdot \log(N) + \\ \beta_5 \cdot \log(DUM_1) + \beta_6 \cdot \log(DUM_2) + \beta_7 \cdot \log(DUm_3) \qquad (0\text{-}2)$$

Table 0-3 shows the result of the 7 variable regression analysis. The correlation coefficient of the model now has value of 0.74, which means that 74% of the variation in the values can be explained by the mathematical model that is

[3] A Dummy variable is a variable that assumes the value 0 or 1(*or 1 and 10 on a log scale*). It is used to indicate the absence or presence, respectively, of a particular qualitative characteristic of the observation.

represented in equation (0-2) (*see appendix e for the interpretation of the regression results*).

Variable	Value	68% (+/-)	90% (+/-)	95% (+/-)	99% (+/-)
β_1	0.826641	0.500328	0.823643	1.000655	1.288283
β_2	4.284427	1.058317	1.742209	2.116634	2.725037
β_3	-13.80574	2.518996	4.14679	5.037992	6.486109
β_4	1.828344	0.41644	0.685547	0.83288	1.072282
β_5	-1.449862	0.624044	1.027307	1.248089	1.606838
β_6	-5.198475	0.599549	0.986982	1.199098	1.543766
β_7	1.4292	0.638774	1.051555	1.277548	1.644766

Table 0-3 Result of 7 variable regression

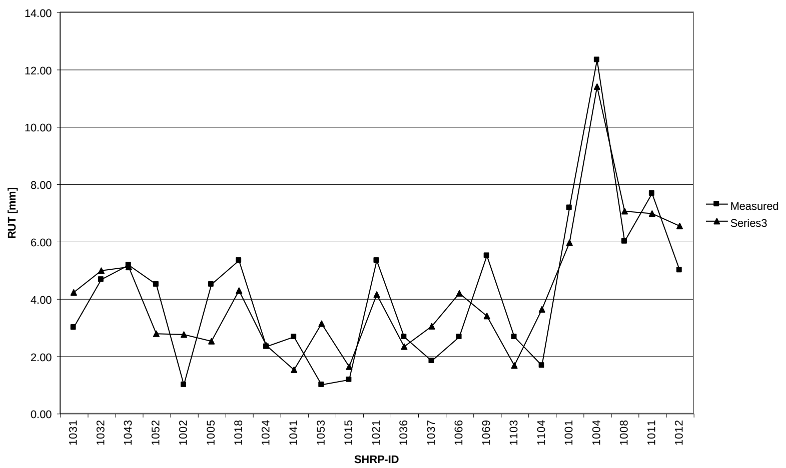

Figure 0-5 Measured and predicted rut per section

Hypothesis testing tests the significance of the regression parameters. This method is useful for testing all of the regression parameters at once. The hypothesis to be tested goes as follows:

$$H_0 : \beta_1 = .. = \beta_7 = 0 \quad against \quad H_1 : \beta_1 = .. = \beta_7 \neq 0$$

The testing is done using the *F-value* from the regression analysis and the so-called *F-tables*. The *F-value* is calculated using equation *(0-3)*.

$$F = \frac{\left[\dfrac{\sum (Y_i - \widehat{Y})^2}{\deg rees\ of\ \ freedom}\right]}{\left[\dfrac{\sum (Y_i - \overline{Y})^2}{error \deg rees\ of\ \ freedom}\right]} \qquad \textit{(0-3)}$$

Where: Y_i = measured rut-depth [mm],

$\widehat{Y}$ = Calculated rut-depth [mm],

$\widehat{Y}$ = Average of rut depth for the samples [mm],

Degrees of freedom = the number of variables that are used in the regression model,

Error degrees of freedom = number of samples – number of regression parameters.

The regression model has an *F-value* of 6.32 that corresponds with a *p-value* of 0.01. If we chose a level significance to either except or drop the *null-hypothesis* of p = 0.05 it would mean that the one or more of the regression parameters are significant to the model.

The model is now accurate enough to be used in the evaluation of the dynamic vehicle loading on rut development.

5.3 Evaluation of the regression model

5.3.1 Relation with SD_{force}

The first relationship to be tested by the model is the one concerning the variation of the axle loads. Testing is done by keeping three of the four variables in the regression constant while increasing the standard deviation of the axle load.

SD_{force} = variable, D_0 = 300 [μm], *AGE* = 7 [years], *N* = 3.000.000

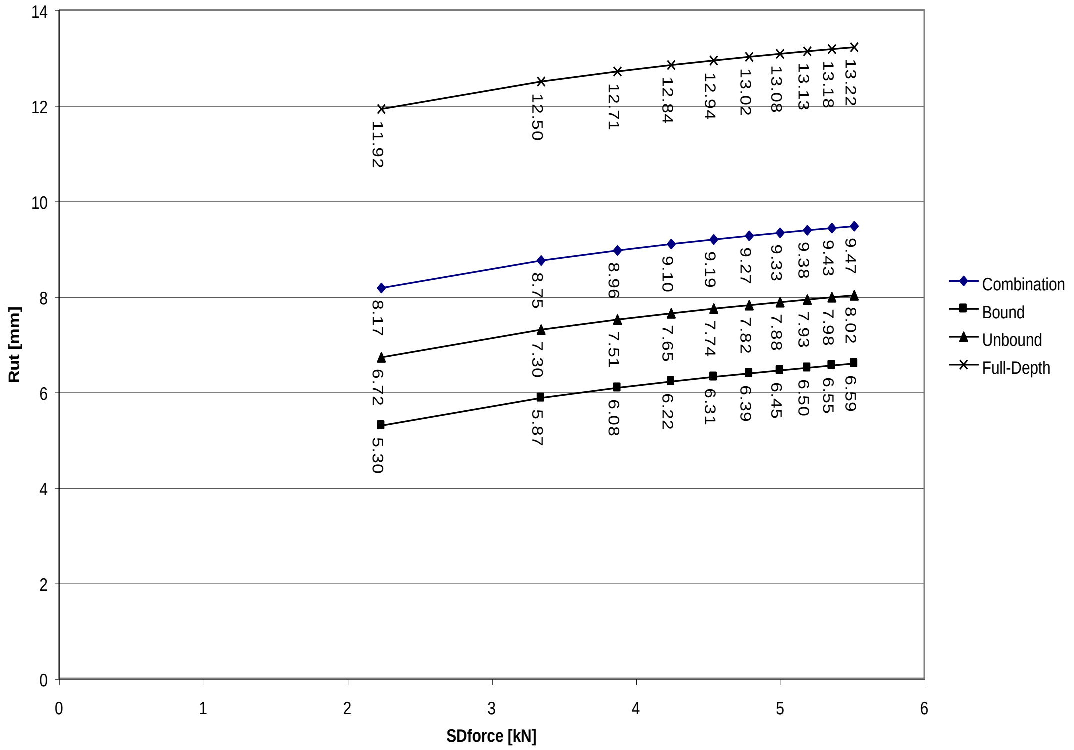

Figure 0-6 variation of SD_{force}

Figure 4-6 shows a trend that could be expected from the theoretical mechanistic models that are commonly used to calculate rut–depth, Rutting increases as the applied load increases. This means that the model is physically correct for the applied force and this data set.
The rut-depth increase is the same for all the models and is approximately 1[mm]. Translating the standard deviation of the axle load using equation *(0-7)* shows that the *IRI* value increases from 1 to 2 which is exactly the range in which most of the test-section fall.
Based on these findings one could state that the increase of the unevenness of the pavement does not significantly effect the average rut on the pavements in this data set.

5.3.2 Relation with D_0

D_0 is seen as a parameter that can be used to describe the bending stiffness of the pavement structure as a whole. An increase in the value of D_0 would indicate a structure that has a smaller bending stiffness and thus is less resistant to rutting.

IRI = 1.6 [m/km] , D_0 = variable, AGE = 7 [years], N = 3.000.000

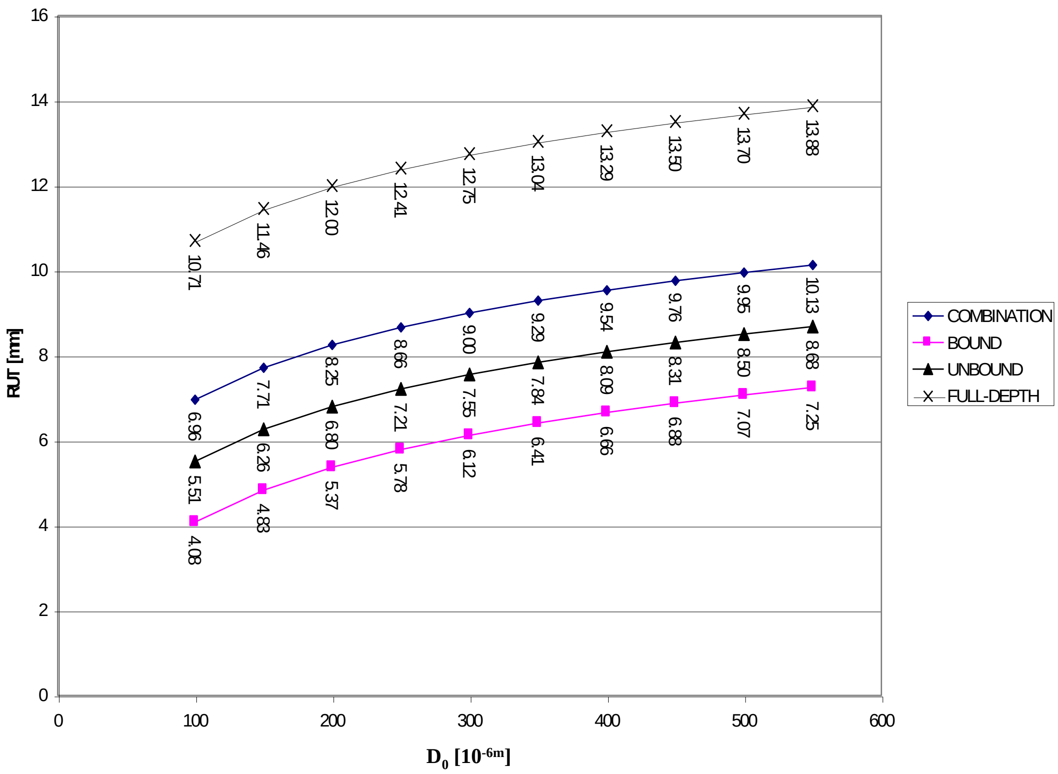

Figure 0-7 Variation of D_0

Figure 4-7 agrees with the proposed relationship between D_0 and rut development. The model predicts a gain of 3.17 [mm] of extra rutting if the D_0 gained about 450[μm].

5.3.3 Relation with the Number of Load repetitions

The variance of the number of load repetitions is the variable that is to be analyzed in the following paragraph. The different points in the plot represent separate roads that have the same mechanistic properties and age but vary in the number of induced load repetitions. The model predicts that the absolute rut-depth increases as the number of load repetitions on the pavement increase.

IRI = 1.6 [m/km], D_0 = 300 [μm], AGE = 7 [years], N = variable

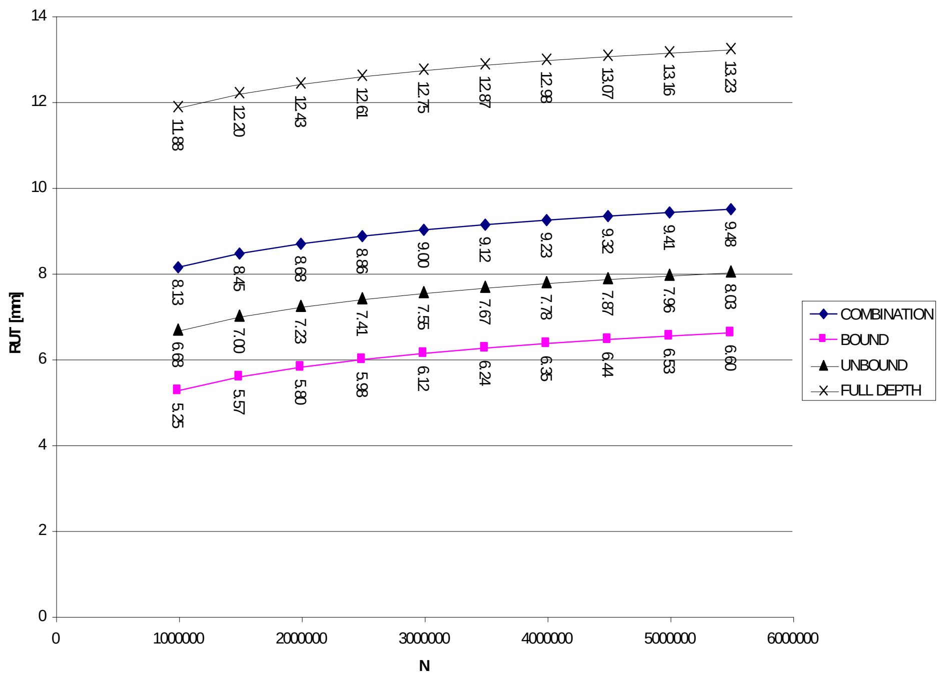

Figure 0-8 Variation of Load repetitions

The relationship that is found for load repetitions and rut-depth corresponds well with earlier models, where it was found that the log-log slope of the rut-depth relation varied between 0.66 and 0.79. The slope of the relation from Figure 0-8 is established to be 0.79 that corresponded well with the rut-development of modified dense asphalt concrete that was used in the Delft University Circular Test Track [8].

5.3.4 Variation of Age

Now the influence of the age of the pavement on the deterioration in terms of rutting will be examined. The plot is generated using the same variable values as the in the other cases, but now the age is varied between 3 to 7 years.

IRI = 1.6 [m/km], D_0 = 300 [µm], *AGE* = variable, *N* = 3.000.000

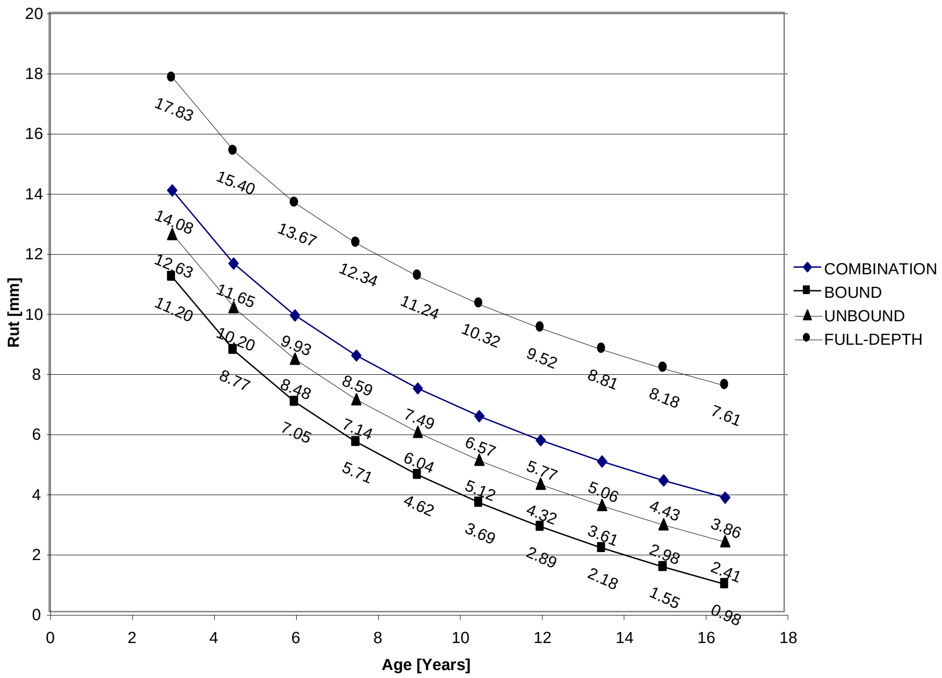

Figure 0-9 Variation of the overlay age

Varying the age results in a surprising strong relationship between age and rut-development. The model suggests that two pavement structures could have a difference 10[mm] in absolute rut-depth if they reach the same level load repetitions within 14-year of each other.

The strong influence of age on rut-depth can be explained using the following example.Figure 0-10 shows a fictitious development of the resistance of the pavement to permanent deformation. As the asphalt on the road ages, the asphalt mix gets stiffer due to the process called “*aging*”. The stiffening of the asphalt also leads to a material that is more resistant to permanent deformation. Figure 0-11 shows the cumulative number of vehicle passages on 3 different roads that reach the same level of load repetitions at different stages of their lifetime. If the two figures are combined to represent the total damage to the road, it becomes obvious that the pavement that has the larger traffic intensity in the early stages of the pavement life will show the largest absolute rut depth.

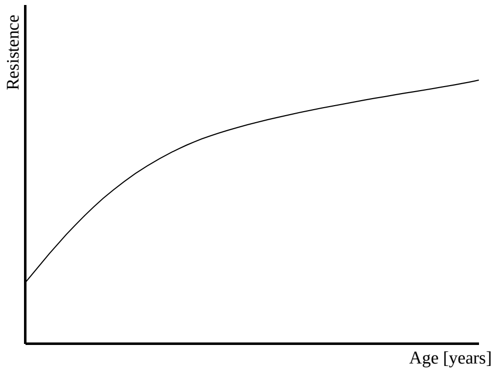

Figure 0-10 Resistance to permanent deformation versus age

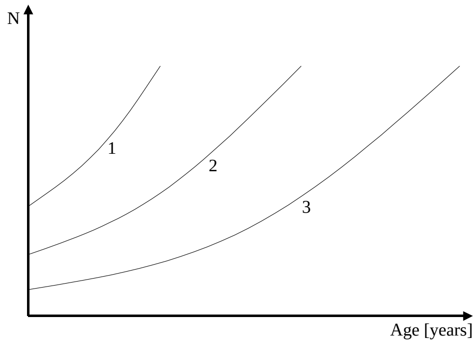

Figure 0-11 Traffic Intensity versus age

The actual relationship between the overlay age and rut-development will probably not be as steep as the one shown in Figure 0-8. The model's prediction is based on the assumption that the mechanistic properties of the road is the same although the age of the different roads varies from 3 to 17 years. Figure 0-12 shows both the trends for a constant D_0 and varying D_0. The deflection under the Falling Weight will probably increase as the asphalt mix stiffness deteriorates[4] leading to an increase of the absolute rut-depth.

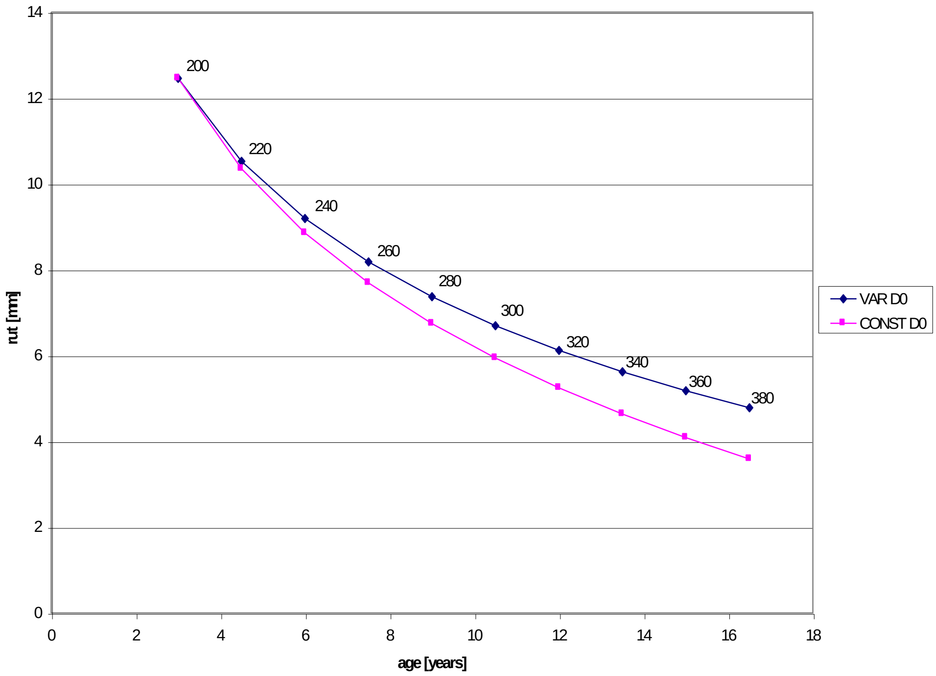

Figure 0-12 variation of both D_0 and Age

[4] Deterioration can be defined as the decrease of the pavement structure's stiffness as a result of increasing damage caused by fatigue of the structure.

5.3.5 Subgrade Strain Criterion

In the PDMAP pavement design computer program a relationship is used for the prediction the rate of rutting that uses the maximum deflection measured by the FWD apparatus as an explaining variable. A similar model was developed to predict the number of load repetitions and corresponding deflection needed to predict 18mm of rut. The relationship was developed for a road with an *IRI* value of 1 and an overlay age of 1[years] on various base materials.

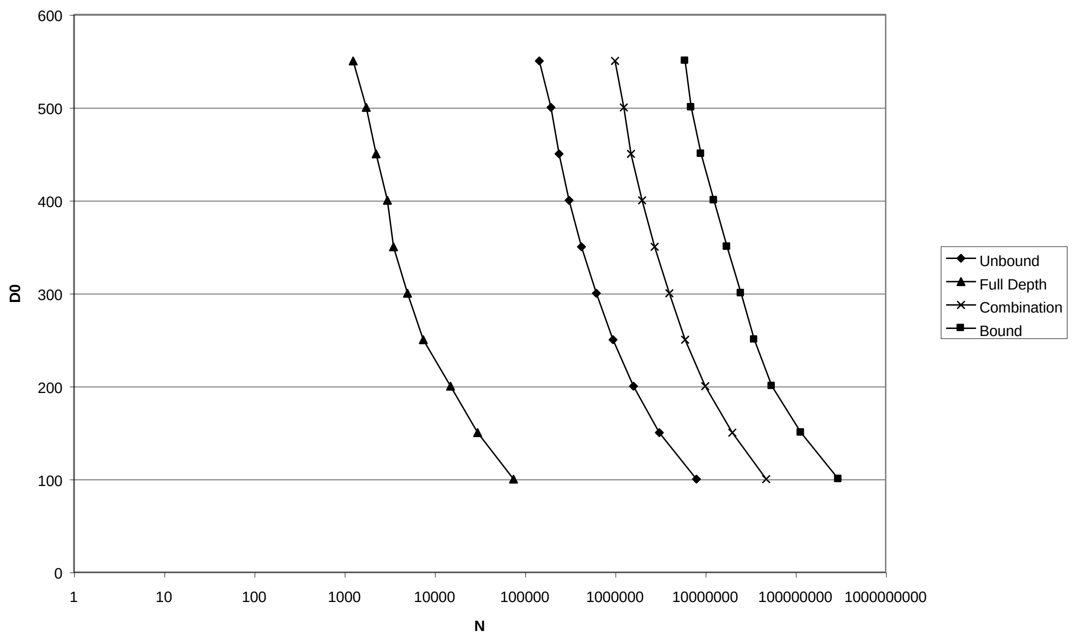

Figure 0-13 constant rut with varying Nequ and D0

A relationship as presented in equation *(0-4)* was fitted to the lines.

$$D_0 = a \cdot N^b \qquad (0\text{-}4)$$

The variables *a* and *b* are calculated for every type of base material (*see* Table 0-4).

Base	A	B
Combination	88.377	-0.42
Bound	474.871	-0.42
Unbound	231.316	-0.42
Full Depth	11.808	-0.42

Table 0-4 a and b values

The *a*-values indicate the sensitivity of the pavement structure to rutting, while the *b*-value indicates the increase in damage as the number of vehicle load repetition increase. The *a*-values show the same trend in rut development as in the previous paragraphs that the full-depth pavement structure or much more sensitive to rutting then the bound pavement structures. The *b*-value indicates the sensitivity of the pavement structure to the increase in loading. The values that are found in this study are constant regardless of the type of pavement structure. This result corresponds well with the findings from the AASHTOO where it was found that the increase in damage is inversely related to the fourth power of the axle load. In this case the damage is related by the applied force to the power of 2.5

5.4 Conclusion on Rut Depth Model

The following conclusions can be drawn from the rut-depth model:

- An increase of the IRI value will not result in a drastic increase in rut development for the test section in this study,

- The age of the pavement overlay has the greatest influence on the development of rutting on the pavements of this sample.

- The rutting mechanisms are greatly dependent on the base material that is used in the pavement structure, hence the use of the "*Dummy variables*".

- The maximum deflection that is measured by means of the Falling Weight Deflectometer can be used as an indication of the pavement's resistance to rutting.

CHAPTER 6 RUT-DEPTH VARIATION MODEL

This chapter will deal with the development and analysis of a mathematical model that is designed to calculate the standard deviation of rutting. The rut-depth variation model would make it possible to predict the error in the rut prediction from 0.

6.1 Selection of variables

A model for the calculation of the average rut-depth was already presented in Chapter 4. The data set that is used in the development of the rut depth model will also be used in the development of the rut-depth-variation-model. The variation of rutting is probably the result of the variation in the pavement/stress conditions of the whole pavement structure. D_0 is considered as an indicator of the pavement and stress conditions (*see chapter 5.1.1*) of pavement so logically the variation of D_0 (*Standard deviation of D_0*) should be indicative of the variations of the pavement. Age is again added to the relation to account for the environmental influences of to the asphalt material. Again the standard deviation of the dynamic vehicle loading and the number of vehicle passages are added to the model to describe the loading of the pavement. The difference with the previous absolute rut-depth-model is addition of the average rut-depth as an independent variable. The reason for this addition is that it is expected that the variation of the rut-depth and the absolute rut-depth will develop as is shown in figure 0-1. It is expected that the variation in the absolute rut-depth will increase as the average rut-depth increases.

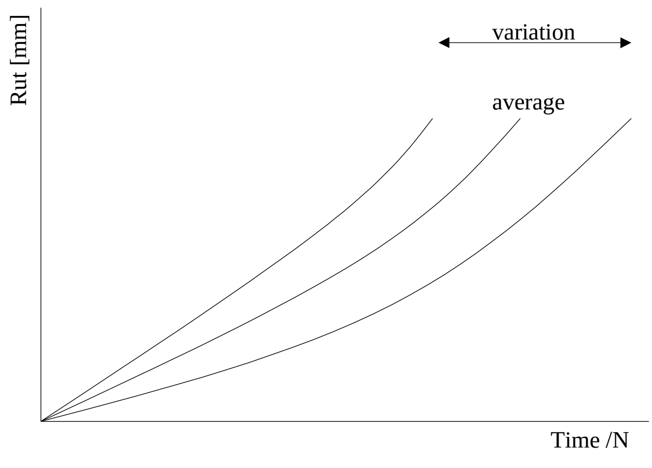

figure 0-1 Variation of rut

The following five variables are used the regression analysis:
The standard deviation of the dynamic vehicle loading, the standard deviation of D_0, the age of the pavement overlay , the number of vehicle passages and the average rut-depth.

6.2 Rut-depth variation model

The samples from the data set are to be fitted to a log-linear mathematical model as shown in equation *(0-1)*. This model is a further development of the model used in chapter 4 and like this model it also resulted in the highest accuracy.

$$STDEV\_RUT = \beta_1 \cdot \log(STDEV\_F^4) + \beta_2 \cdot \log(STDEV\_D_0) + \beta_3 \cdot \log(AGE) + \beta_4 \cdot \log(N) + \beta_5 \cdot \log(AVE\_RUT) \quad (0\text{-}1)$$

Where: *STDEV_RUT* = standard deviation of the rut [mm],
STDEV_F = the *IRI* value of the test –section [m/km],
$STDEV\_D_0$ = standard deviation of D_0 [10^{-6}m],
AGE = age of the pavement overlay [years],
N = number of vehicle passages,
AVE_RUT = average rut [mm].

The samples are used as an input to the software program DataFit© that uses the method of the "*least-squares*" to determine the regression parameters.

Variable	Value	68% (+/-)	90% (+/-)	95% (+/-)	99% (+/-)
β_1	0.095996	0.518611	0.853742	1.037223	1.335361
β_2	0.493297	0.81701	1.344969	1.634021	2.103703
β_3	0.742031	2.203568	3.627531	4.407136	5.673921
β_4	-0.153884	0.307237	0.505776	0.614474	0.791097
β_5	0.541467	0.757607	1.247178	1.515214	1.950746

Table 0-1 regression parameters for rut-variation model

The regression analysis found a correlation coefficient of 0.57, which means that 57% of the variations of the sample. Figure 0-2 shows that the predicted value and the measured value seem to correlate well.

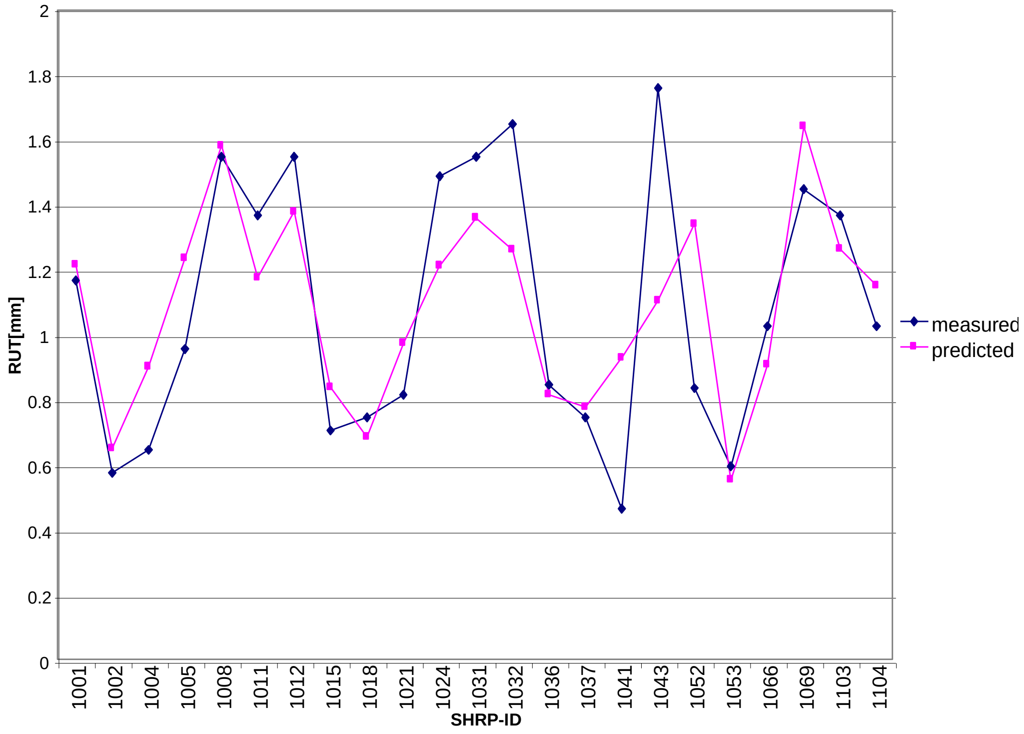

Figure 0-2 measured versus predicted ut depth variation

A preliminary conclusion that can be made on from this model is that the base material does not seem have any significant effect on variation in rut-depth, hence the lack of "*dummy*" variables.

6.3 Evaluation of the rut-depth variation model

The following paragraphs will deal with the relationship between the rut-depth variance and on of the regression variables while keeping the other four variables at a constant level.

6.3.1 Relation with the variation in vehicle loading

In this chapter the standard deviation of the axle loading value is varied while the other four variables are kept at constant values. It is expected that the variation of the rut-depth will increase as the unevenness of the pavement worsens.
The plot is generated using the following values for the four other variables:

Standard deviation of D_0 = 15.00 [μm], Age = 7 [years],
Number of vehicle passages = 3.000.000 and average rut = 5.00 [mm].

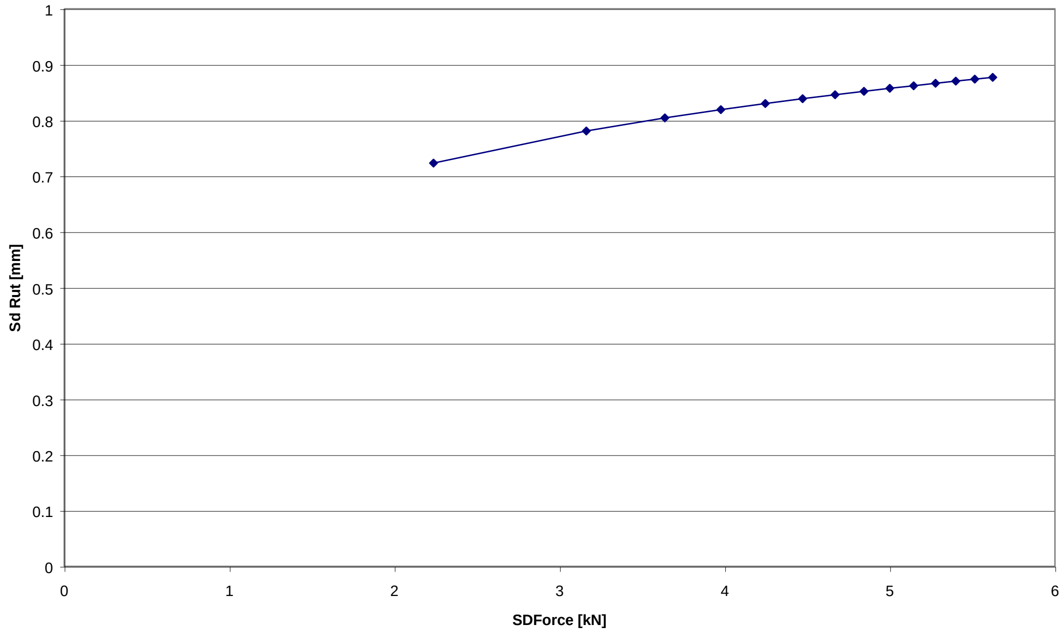

Figure 0-3 Variation of IRI

Figure 0-3shows the behavior that was expected, namely that the variation will increase as the *IRI* increases. The reader should note however that the increase is very small. If the *IRI* gains 2 points, the rut-depth-variation increases with less then 0.2 [mm], which is negligible effect. If the reader also considered the fact that the test section have little unevenness it becomes evident that the increase of the standard deviation of rut has little to no meaning at all.

6.3.2 Relationship with the standard deviation of D_0

The next variable to be varied is the standard deviation of D_0. The relation that is to be expected is the same as the one for the variation of D_0 (*see chapter 5.3.2*), namely an increase in Standard Deviation of D_0 will lead t an increase in the rut-depth variation. The values that were used for the other four variables to derive the figure below are:

IRI= 1.6, Age = 7 [years], Number of vehicle passages = 3.000.000 and
Average rut = 5.00 [mm].

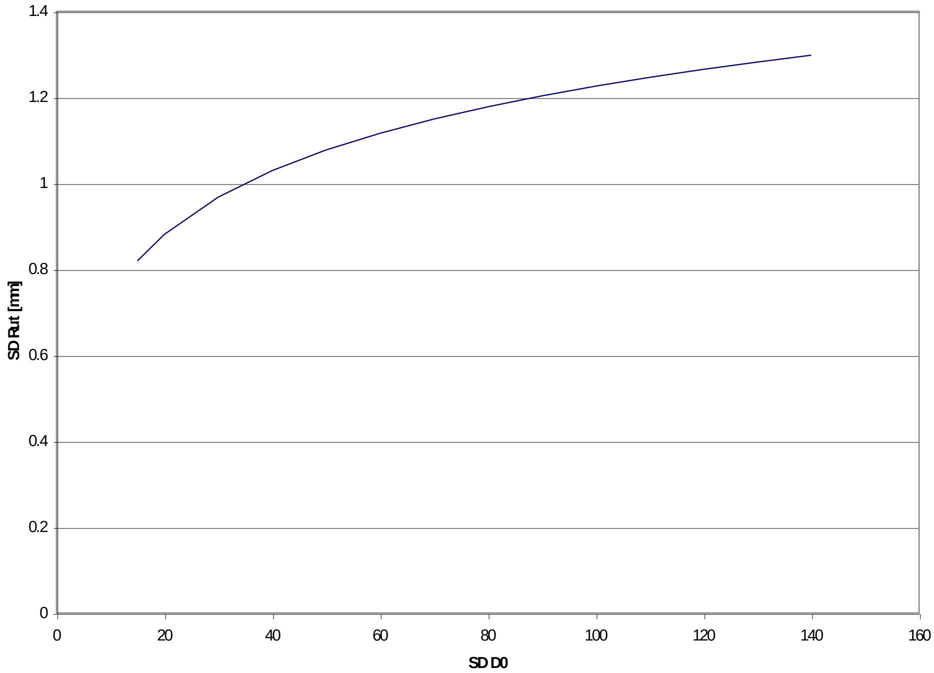

figure 0-4 Variation of Standard Deviation D_0

The result is given in figure 0-4, which shows that the previous assumption is correct. The gain in standard deviation is about 0.5 [mm] if the standard deviation of D_0 is varied from 20 to 140 [µm].

6.3.3

Relationship with the Overlay Age

This paragraph will investigate the relationship between the age of the overlay and the development of the error in rut prediction. The relationship is evaluated by keeping four of the five regression parameters constant (*see below*) while increasing the age of the material. The result of this evaluation is shown in figure 0-5.

IRI= 1.6, Standard Deviation D_0 = 15 [μm],
Number of vehicle passages = 3.000.000 and Average rut = 5.00 [mm].

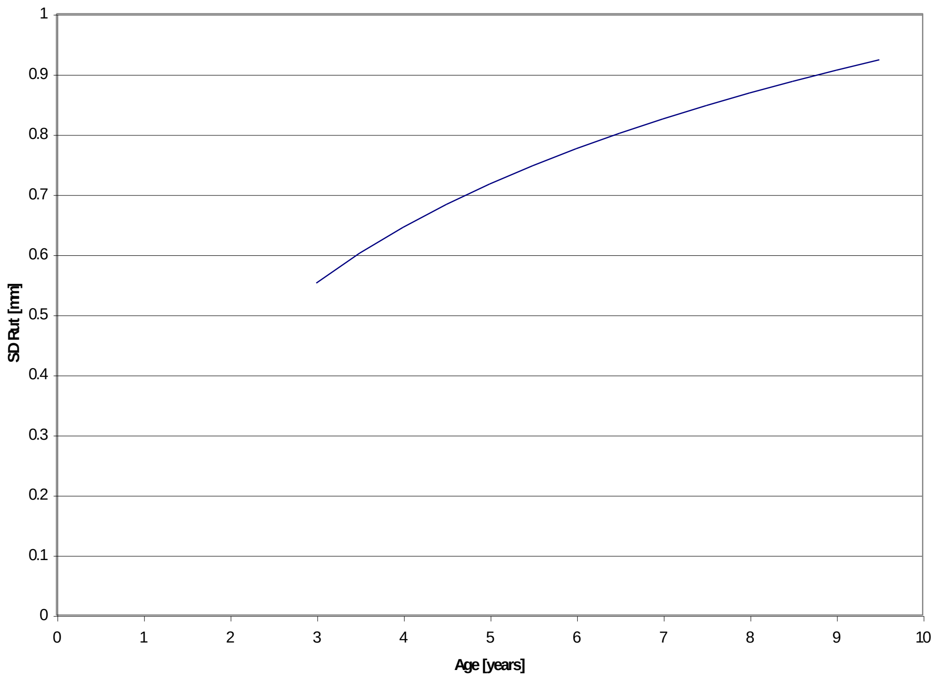

figure 0-5 Variation of Overlay Age

There is a positive relationship between the age and the variation in the rut-depth that would indicate that the material properties that are influenced by age also show an increased variation. One should also note that again the relationship with age is a very strong one as was found in the average rut-depth model of the previous chapter.

6.3.4

Variation of the number of vehicle Passages

This paragraph will deal with the relationship between the number of vehicle passages and the development of the standard deviation of the average rut-depth. The same method is used as in the previous paragraphs.

IRI= 1.6, Standard Deviation D_0 = 15 [μm],
Age = 7 years and Average rut = 5.00 [mm].

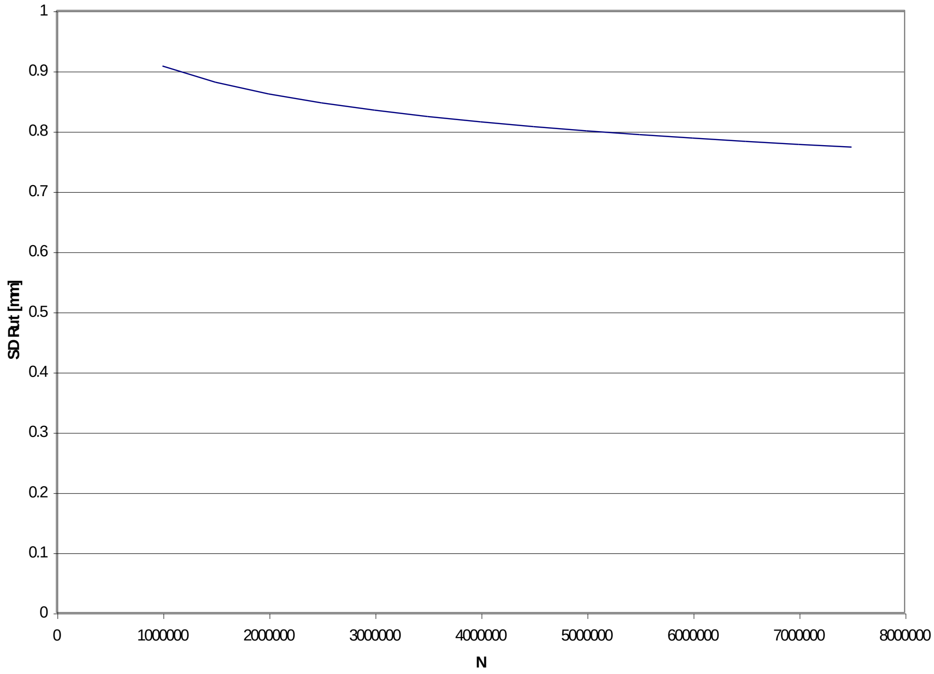

Figure 0-6 relationship between N and SD_{rut}

The result of the evaluation shows a decrease in the standard deviation of rut as the number of vehicle passages increase. The relationship can be explained in one would consider the implication of an increase in the number of vehicle passages while keeping the average rut-depth constant. It would mean that the road with a grater number of vehicle passages is better resistant to rut development. This means that the pavement is of a higher quality thus has less variation in the material properties hence the above-mentioned relationship.

6.4 Conclusions

The following conclusions can be drawn from the research of this chapter:

- The standard deviation of the average rut-depth is most strongly related to the age of the pavement and the average rut-depth itself.
- The standard deviation of the rut-depth does not show any dependency on the type of base used in the pavement structure hence has no relationship with the stress condition in the pavement.

Bill Waterson

CONCLUSIONS

This research project was focused on finding the effect of dynamic vehicle loading on the rut development of in-service pavements using data obtained from test-section that are frequently monitored by the SHRP-NL project group. The following conclusions are drawn as a result of this study.

- Vehicle simulations showed that the *IRI* value is a good indicator for the variation in the axle load. The standard deviations of the loads have a linear relationship with the *IRI* value.
- The speed of the vehicle has a negligible effect on the dynamic vehicle load. This conclusion can be drawn for only this sample; as the longitudinal unevenness of the test-sections is small, the variations in the axle load will be small and thus the variations between vehicles travelling at different speeds. Thus simulating at one speed will suffice.
- Based on the sample, the dynamic vehicle loading has no effect on rut development. This is due to the fact that the unevenness of the test-sections that area used in this study are very smooth so the increase in axle loads is marginal.
- The regression analysis also showed that rut development has a great dependency on the type of base material used in the pavement structure. Since the type of base influences the stress conditions in the asphalt layer and the subgrade one could state that the rut development is strongly dependent on the stress conditions in the pavement structure.
- The regression analysis also showed a strong relationship with the age of the overlay. The model showed that two sections that have the same level of traffic loading but differ in the time they took to obtain that level of loading will have a rather large difference in the absolute rut-depth.
- The standard deviation of the rut-dept is not influenced by the type of based that is used in the pavement structure.
- The standard deviation of the rut depth predicted very small values, most of the time even smaller then could be measured using the method used by SHRP-NL.

Bill Waterson (1986)

FUTURE RECOMMENDATIONS

The recommendations that are mentioned in this part of the report are aimed at further research in this field.

Rut depth predictions are influenced by the uncertainties that are introduced in the model as a result of assumptions that are made. Most rut prediction models assume that the material, loading and pavement properties are constant in both longitudinal as transverse directions. In-service pavements however will show a variation in all of these parameters. The only way of establishing a good relationship between dynamic vehicle loads and rut development is by eliminating the scatter caused by variations in material and pavement properties or increase the scatter caused by the dynamic vehicle loads.

- The scatter caused by variation in material or pavement can be eliminated by adding densification values of the material to the model and by adding detailed layer thickness measurements so these parameters can also used to explain rut.

- Using test sections that have higher degree of unevenness can enhance the influence of the dynamic vehicle loading and thus making it easier to recognize.

Table of authorities

[1] Brown, S.F.and Brunton, J.M.(1982). "The development and implementation of analytical pavement design for British conditions" Proc. 5th Int. Conf. On the Structural Design of Asphalt Pavements, pp. 3-16, NL

[2] Collop, A.C. (1994), "Effects of traffic and temperature on the flexible pavement wear", Dissertation for the degree of Doctor of Philosophy, University of Cambridge, Dep. of Engineering, UK.

[3] Eisenmann, J. and Hilmer, A. (1978)" Influence of wheel load and inflation pressure on the rutting effect at asphalt-pavements-experiments and theoretical investigations" Proc. 6th Int. Conf. on the Structural Design of Asphalt Pavements, Ann Arbor, pp.392-403, Mi, USA.

[4] Eisenmann J.(1975) "Dynamic wheel load fluctuations- road stress". Strasse und Autobahn, Vol. 4, pp 127-128, DE..

[5] Van Gurp, C.A.P.M., "Characterization of Seasonal Influences on Asphalt Pavement Properties with the use of Falling Weight Deflectometers", 1995, Thesis ISBN 90-9008036-8, Road and Railroad Research laboratory of Delft University of Technology, Delft, NL.

[6] Huurman, M. (1997). "Permanent deformation in concrete block pavements", dissertation for the degree of Phd., Delft University of technology, Faculty of Civil Engineering, Road and Railroad Research Laboratory, Delft, NL

[7] Iman, R.L. and Conover, W.J.(1983), "Modern Business Statistics", ISBN 0-471-50024-0, John Wiley & Sons, 2nd ed.,new York, USA.

[8] Molenaar, A.A.A. (1994), "Structural Design of Pavements, Part III Design of Flexible Pavements", Lecture notes, Road and Railroad Laboratory of the Delft University of Technology, Delft, NL.

[9] -- Road Construction Manual – Pavement design (3rd ed.) (in Dutch),1994, Rijkswaterstaat, Dienst Weg en Waterbouwkunde, DWW, Delft, NL.

[10] Sweatman, P.F. (1983),"A Study of Dynamic Wheel Forces in Axle Group suspensions of Heavy Vehicles"ARRB special report, no. 27/83, Australian Road Research Board, Australia.

[11] Verhasselt, A.F. and Choquet, F.S. (1993). "Comparing field and laboratory aging of bitumens on a kinetic basis", Proc., 72nd Annual Meeting, Transportation Research Board, Washington D.C., USA.

Appendix a International Roughness Index (IRI)

Resource:
http://www.umich.edu/~glcttr/HomePage.html
http://www.umich.edu/~glcttr/HomePage.html

International Roughness Index (IRI)

This page describes the International Roughness Index (IRI) used to describe road roughness. It is part of a set of Web pages related to road roughness, and is provided as a service by the Engineering Research Division (ERD) of The University of Michigan Transportation Research Institute (UMTRI).

Background

Almost every automated road profiling system includes software to calculate a statistic called the International Roughness Index (IRI). Since 1990, the Federal Highway Administration (FHWA) has required the states to report road roughness on the IRI scale for inclusion in the Highway Performance Monitoring System (HPMS).

The IRI was proposed by The World Bank as a standard roughness statistic.

The World Bank sponsored several large-scale research programs in the 1970's that investigated some basic choices facing developing countries: should the governments borrow money to build good, expensive roads, or should they save money with poor, cheap roads? It turns out that poor roads are also costly to the country as a whole, due to user costs such as damage to vehicles. Road roughness was identified as a primary factor in the analyses and trade-offs involving road quality vs. user cost. The problem was, roughness data from different parts of the world could not be compared. Even data from the same country were suspect because the measures were based on hardware and methods that were not stable over time.

In 1982, the World Bank initiated a correlation experiment in Brazil to establish correlation and a calibration standard for roughness measurements. In processing the data, it became clear that nearly all roughness measuring instruments in use throughout the world were capable of producing measures on the same scale, if that scale were suitably selected. From that point on, an objective of the researchers was to develop the IRI.

The IRI is reproducible, portable, and stable with time.

The IRI is the first widely used profile index where the analysis method is intended to work with different types of profilers. It is defined as a property of the true profile, and therefore it can be measured with any valid profiler. The analysis equations were developed and tested to minimize the effects of some profiler measurement parameters such as sample interval. Example computer programs were published by The World Bank and have been used by profiler developers and others to test new software that computes IRI.

The IRI simulates a standard vehicle with a perfect road meter.

At the time of its development, response-type road roughness measuring systems were common, so the index was tailored to correlate well with the output of these systems. The filter in the IRI is based on a mathematical model called a quarter-car. The quarter-car filter calculates the suspension deflection of a simulated mechanical system with a response similar to a passenger car. The simulated suspension motion is accumulated and divided by the distance traveled to give an index with units of slope (m/km, in/mi, etc.).

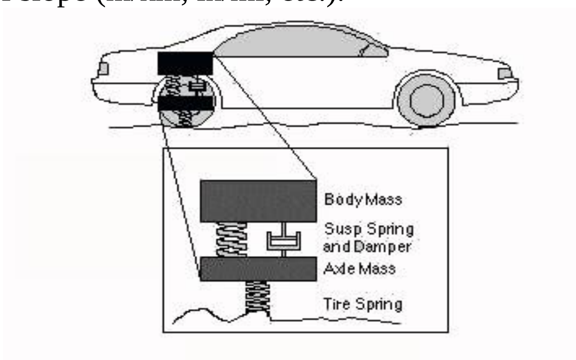

Much of the research underlying the IRI was funded by the National Cooperative Highway Research Program (NCHRP). The IRI is based on the "Golden Car" described in NCHRP Report 228.

Properties of the IRI Analysis

The quarter-car model used in the IRI algorithm is just what its name implies: a model of one corner (a quarter) of a car. The model is shown schematically in the above figure: it includes one tire, represented with a vertical spring, the mass of the axle supported by the tire, a suspension spring and a damper, and the mass of the body supported by the suspension for that tire.

The quarter-car model was tuned to maximize correlation with response-type road roughness measuring systems.

This quarter-car simulation is meant to be a theoretical representation of the response-type systems in use at the time the IRI was developed, with the vehicle properties adjusted to obtain maximum correlation to the output of those systems. Considerations in its design are described in NCHRP Report 228. The model was called "The Golden Car" at the time, because it was intended to serve as a reference for response-type systems.

The parameters used in the quarter car give it simulated response properties typical of most highway vehicles with one exception: the damping is higher than most cars. This keeps the IRI from "tuning in" to certain wavelengths and degrading correlation with other vehicles. The figure below shows how IRI values from profile data relate to raw measures from a response-type system.

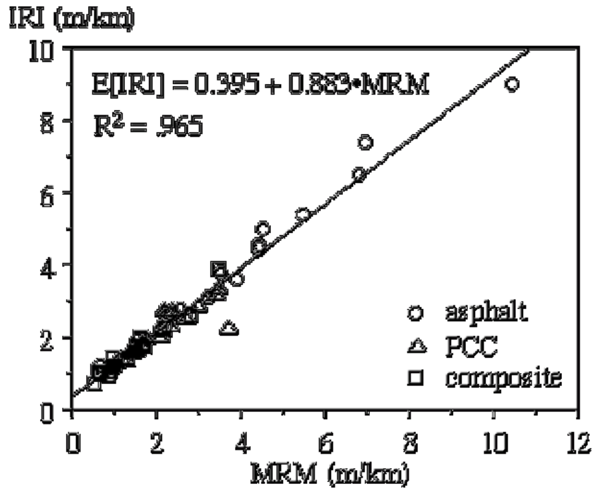

The IRI describes profile roughness that causes vehicle vibrations.
The response of the IRI to sinusoids is intentionally very similar to measured physical response of highway vehicles. It was mainly developed to match the responses of passenger cars, but subsequent research has shown good correlation with light trucks and heavy trucks. The IRI has become recognized as a general-purpose roughness index that is strongly correlated to most kinds of vehicle response that are of interest. Specifically, IRI is very highly correlated to three vehicle response variables that are of interest:

1. road meter response (for historical continuity),
2. vertical passenger acceleration (for ride quality), and
3. tire load (for vehicle controllability and safety).

The IRI is not related to all vehicle response variables. For example, it does not correlate well with vertical passenger position, or axle acceleration.
The fact that IRI correlates well with both road meter response and passenger acceleration is no coincidence: the correlation between road meter response and passenger acceleration was certainly a factor in the decades of acceptance of the road meter as a useful tool for measuring roughness.
IRI is influenced by wavelengths ranging from 1.2 to 30.5 m (4 to 100 ft).
The wave-number response of the IRI quarter-car filter is shown in the next figure. The amplitude of the output sinusoid is the amplitude of the input, multiplied by the "gain" shown in the figure. The gain shown in the figure is dimensionless. Thus, if the input is a sinusoid with amplitude that is slope, the output is the product of the input amplitude and the value taken from the plot.

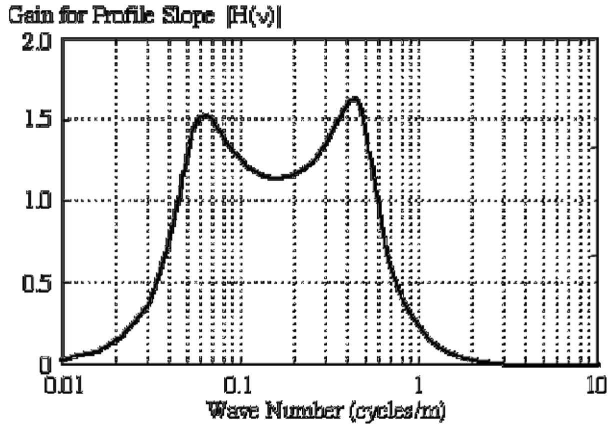

The IRI filter has maximum sensitivity to slope sinusoids with wave numbers near 0.065 cycle/m (a wavelength of about 15.4m) and 0.42 cycle/m (a wavelength of about 2.4 m). The response is down to 0.5 for 0.033 and 0.82 cycle/m wave numbers, which correspond to wavelengths of 30.5 m and 1.2 m, respectively. However, there is still some response for wavelengths outside this range.

The IRI scale is linearly proportional to roughness.

If all of the elevation values in a measured profile are increased by some percentage, then the IRI increases by exactly the same percentage. An IRI of 0.0 means the profile is perfectly flat. There is no theoretical upper limit to roughness, although pavements with IRI values above 8 m/km are nearly impassable except at reduced speeds.

The IRI was the first highly portable roughness index that is stable with time.

The IRI is not the first profile-based roughness index. When it was introduced, profilers from different countries and different manufacturers were each used with profile analyses developed for their specific hardware. Most of the analyses were not intended to work with true profile. Those that did had specific requirements for the interval between elevation measures, and gave significant errors when applied to profiles that had a different interval.

The software published by The World Bank was tested by new users, who found that under controlled research tests, they could obtain nearly identical IRI values using different profilers.

Definition of the IRI

The above descriptions of the IRI background and properties are intended to give an idea of what the IRI computer software is intended to simulate, and how you can interpret the IRI scale. However, the IRI is rigorously defined as a specific mathematical transform of a true profile. The specific steps taken in the computer program to compute IRI are listed below.

The IRI is calculated for a single profile.

If your profiler measures several profiles simultaneously, then you can get the IRI for each. The IRI standard does not specify how you locate the line on a road that defines the profile. Any possible line on the ground has an associated IRI statistic.

The standard does not specify how you combine IRI values for different profiles taken for the same road. They can be averaged, but the result is not IRI--it is the average of several IRI's.

The profile is filtered with a moving average with a 250-mm base length.

The moving average is a low-pass filter (it attenuates short wavelengths) that smoothes the profile. It has no effect unless the profile sample interval is shorter than 167 mm (6.6 in).

The 250-mm moving average filter should be omitted for profiles obtained with some systems.

This step should be omitted if the profile has already been filtered by a moving average or with an anti-aliasing filter whose cut-off attenuates wavelengths shorter than 0.6 m. Profilometers by K.J. Law detect elevation values at intervals of 25.4 mm, apply a 300 mm moving average filter, and store the result at 152.4-mm intervals. It is important to skip the 250-mm filter when processing profiles from these systems.

The profile is further filtered with a quarter-car simulation.

The quarter-car parameters are specified as part of the IRI statistic, and the simulated travel speed is specified as 80 km/h (49.7 mi/h). The output of the filter represents suspension motion of the simulated quarter car.

The filtered profile is accumulated by summing absolute values of the filtered point, and divided by the profile length.

The resulting IRI statistic has units of slope. As a user, you can express the slope in any appropriate units. The most common choices are in/mi and m/km (1 m/km = 63.36 in/mi).

Summary: IRI is a profile index.

The IRI is a specific profile index. The analysis is applied to a single profile, the profile is filtered (twice), the filtered result is accumulated, and finally divided by the length of the profile. The IRI is linearly related to variations in profile, in the sense that if all of the elevation values in the profile are doubled, the resulting IRI will also be doubled.

Appendix b The ASTM 1170-91 Standard

Appendix c Overview of the SHRP-NL Test-sections

Appendix d Inspection Form

Appendix e Interpreting the regression analysis

Interpreting the Results

When determining the goodness of fit of the model(s), the following points should be examined:

1. Check the solution convergence. Each iterative step of the nonlinear solver returns the best estimate found so far in the solution process. After each iteration, the merit function is compared to that from the previous iteration. Since the solver returns the best estimates reached so far, the newly computed merit function will either be better (lower) or unchanged. So as to not run on indefinitely, we stop the process if the difference in the merit function between iterations reaches a reasonable specified Regression Tolerance, a Maximum Number of Iterations, or a Maximum Number of Unchanged Iterations. By viewing the Solution Log or the Solution itself, you can see which of the limits ceased the iterations for a particular model. If the solution reached the Maximum Number of Iterations, you may check to see if the merit function was steadily decreasing and increase the allowable number of iterations. The default values are typically adequate, but DataFit gives you the capability to alter them to your possibly special needs.

2. Check to see how well the model describes the actual data. This information can be obtained by the following calculated parameters.

a) Residuals are the vertical differences between the curve created by the fitted function and the actual data point. If the residual is positive, the estimated value lies below the actual data point. If the residual is negative, the estimated value lies above the actual data point. The residuals should be randomly scattered around zero. If there are groups of residuals with like signs, it is probable that another functional approximation exists that would better describe the data.

b) The Residual Sum of Squares (RSS), is the sum of the squares of the differences between the entered data and the curve generated from the fitted model. A perfect fit would yield a residual sum of squares of 0.0.

c) The Residual Standard Deviation (RSD), is the standard deviation of the differences between the entered data and the curve generated from the fitted model. This gives you an idea about how scattered the residuals are around the average.

d) The Correlation Coefficient (R2), is a measure of the correlation between the dependent and independent variables for the fitted approximation. The value of R2 is typically between 0.0 and 1.0. A value of 1.0 indicates perfect correlation, a value of 0.0 indicates no correlation. If the functional approximation is extremely poor, the value of R2 may lie outside of this range.

e) The Standard Error of the Estimate (Std Err), is a measure of the amount of error in the functional approximation. As the standard error approaches 0.0, you can be more certain that the functional approximation accurately describes the data. A perfect fit would yield a standard error of 0.0.

f) Finally, you can observe a plot of actual vs. estimated data.

3. Check to see if the results are scientifically or statistically meaningful. Does the fitted value of any of the variables violate a possible physical reality? For example, suppose you are fitting a model in which one of the parameters represents electrical resistance and returns a negative value. This probably means that the model you selected is not the correct one.

4. Look at the confidence intervals. The confidence intervals for each variable are reported to you in the Results window for at levels of 68%, 90%, 95% and 99%. Confidence intervals are a means of determining the probability that the fitted variable lies within a certain range. For example, for a 99% confidence interval, you can be approximately 99% sure that the reported value lies within the calculated range. If the confidence is very wide, the fit is not unique, meaning that different values chosen for the variables would result in nearly as good a result. Data containing a lot of scattering, or not collecting a sufficient amount of data would cause the confidence intervals to be excessive, however the most common reason is fitting the data to a model with variable redundancy. In the equation, the variables a and b are indistinguishable. There is no way for the algorithm to determine how to distribute a value (the product of a and b) between these two variables. Also, entering large standard deviations in the spreadsheet would cause the confidence intervals to be wide.

5. It is possible to converge on a false minimum in the merit function. This is a problem inherent in any iterative optimization procedure. Nonlinear regression will assure that once a solution has been obtained, small changes in the variables will worsen the fit. It is rare but possible, however, that some large change may actually converge to a better fit. This problem is rare, except in cases where the data is widely scattered, there were too few data points collected or the model chosen is completely wrong for the data. Determining good initial estimates is important, which is why they are calculated for you in DataFit when performing nonlinear regression. If you think you may have possibly reached a false minimum, you may use the Range feature when specifying the initial estimates. This feature will solve the model with a range of initial estimates, returning the best-fit parameters from the enumerated initial conditions specified.